

ISU  
1993  
CH25  
C.3

A scanning electron microscope study of rat sciatic nerve fiber  
regeneration through silicone rubber single lumen nerve cuffs

by

Yueh-Sheng Chen

A Thesis Submitted to the  
Graduate Faculty in Partial Fulfillment of the  
Requirements for the Degree of  
**MASTER OF SCIENCE**

Interdepartmental Program: Biomedical Engineering  
Major: Biomedical Engineering

Signatures have been redacted for privacy

Iowa State University  
Ames, Iowa

1993

## TABLE OF CONTENTS

<b>1. INTRODUCTION</b>	1
<b>2. LITERATURE REVIEW</b>	4
2.1. Background	4
2.1.1. The mammalian peripheral nervous system	4
2.1.2. Nerve degeneration	4
2.1.3. Nerve regeneration	7
2.2. Repair techniques	10
2.3. Characteristics of the silicone rubber cuffs	12
2.4. Silver staining of nerve tissue	13
2.5. Scanning electron microscopy	14
2.5.1. Secondary electrons	15
2.5.2. Backscatter electrons	15
<b>3. MATERIALS AND METHODS</b>	17
3.1. Samples	17
3.2. Light microscopy and scanning electron microscopy	18
3.3. Quantitative evaluations	19
3.3.1. Quantitative studies	19
3.3.2. Preparation of fiber diameter histograms	23
3.4. Statistical methods	23
<b>4. RESULTS</b>	24
4.1. Microstructure	24
4.1.1. Control	29
4.1.2. Proximal section	29

4.1.3. Middle section	29
4.1.4. Distal section	32
4.2. Fiber diameter histograms	32
4.2.1. Fiber diameter histograms observed using LM	39
4.2.2. Fiber diameter histograms observed using SEM	40
4.3. Quantitative results	43
4.3.1. Quantitative results from LM	56
4.3.2. Quantitative results from SEM	67
<b>5. DISCUSSION</b>	<b>69</b>
<b>6. CONCLUSIONS</b>	<b>74</b>
<b>BIBLIOGRAPHY</b>	<b>76</b>
<b>ACKNOWLEDGEMENTS</b>	<b>82</b>
<b>APPENDIX: FIBER DIAMETER HISTOGRAMS</b>	<b>83</b>

**LIST OF FIGURES**

- Figure 2.1: Schematic representation of the structure of a mammalian peripheral nerve 5
- Figure 4.1: Secondary electron micrograph of a cross-section of the right sciatic nerve at the mid-thigh level from a normal control, (animal #9, 24 weeks). Bodian stain. Scale bar=10  $\mu\text{m}$  25
- Figure 4.2: Backscatter electron micrograph of the identical field as Figure 4.1. Axons are the bright features surrounded by myelin sheaths. Bodian stain. Scale bar=10  $\mu\text{m}$  25
- Figure 4.3: Backscatter electron image of a single-lumen cuff repaired nerve section, (animal #48, middle section, 24 weeks). Category I and category II axons are in the field of view. Bodian stain. Scale bar =10  $\mu\text{m}$  27
- Figure 4.4: Backscatter electron image showing silver grains on the surface for a region of a single-lumen cuff nerve section, (animal #41, middle section, 24 weeks). Some regions of nerve sections were heavily covered with these features whereas even on the same section there were regions with relatively few particles of this type on the surface. Bodian stain. Scale bar=2  $\mu\text{m}$  27
- Figure 4.5: Backscatter electron image of a single-lumen cuff nerve section, (animal #6, proximal section, 24 weeks). Microfascicles are apparent. Category I and category II axons are seen. Bodian stain. Scale bar=10  $\mu\text{m}$  30
- Figure 4.6: Backscatter electron image of a single-lumen cuff nerve section, (animal #6, middle section, 24 weeks). Category I and category II axons are seen. Bodian stain. Scale bar=10  $\mu\text{m}$  30
- Figure 4.7: Backscatter electron image of a single-lumen cuff nerve section, (animal #6, distal section, 24 weeks). Category I and category II axons are seen. Bodian stain. Scale bar=10  $\mu\text{m}$  33

**LIST OF TABLES**

Table 3.1: Implant period, type of repair, animal number, nerve section, and slide number for sections used in the present LM and SEM study	20
Table 4.1: Distributions of percentage of axons within $\pm 1 \mu\text{m}$ of the mean diameter observed using LM	35
Table 4.2: Distributions of percentage of category I axons within $\pm 1 \mu\text{m}$ of the mean diameter observed using SEM	36
Table 4.3: Distributions of percentage of category II axons within $\pm 1 \mu\text{m}$ of the mean diameter observed using SEM	37
Table 4.4: Distributions of percentage of total axons within $\pm 1 \mu\text{m}$ of the mean diameter observed using SEM	38
Table 4.5: Axon counts, reference area and axons per unit area observed using LM	44
Table 4.6: Category I axon counts, reference area and category I axons per unit area observed using SEM	45
Table 4.7: Category II axon counts, reference area and category II axons per unit area observed using SEM	46
Table 4.8: Total axon counts, reference area and axons per unit area observed using SEM	47
Table 4.9: Mean axon diameter, nerve area and percentage of nerve observed using LM	48
Table 4.10: Mean category I axon diameter, nerve area and percentage of nerve observed using SEM	49
Table 4.11: Mean category II axon diameter, nerve area and percentage of nerve observed using SEM	50
Table 4.12: Mean total axon diameter, nerve area and percentage of nerve observed using SEM	51
Table 4.13: Diameter ratio and estimated total axons in each nerve section observed using LM	52

Table 4.14: Category I axon diameter ratio and estimated total category I axons in each nerve cross section observed using SEM	53
Table 4.15: Category II axon diameter ratio and estimated total category II axons in each nerve cross section observed using SEM	54
Table 4.16: Axon diameter ratio and estimated total axons in each nerve cross section observed using SEM	55
Table 4.17: Mean axon diameter comparisons between repaired nerve sections and normal control observed using LM	57
Table 4.18: Mean axon diameter comparisons between nerve sections in the same animal observed using LM	58
Table 4.19: Mean diameter comparisons of the same category of axons in repaired nerve sections and in normal control observed using SEM	59
Table 4.20: Mean axon diameter comparisons between repaired nerve sections and normal control observed using SEM	61
Table 4.21: Diameter comparisons between the category I and the category II axons in the same nerve section observed using SEM	62
Table 4.22: Mean diameter comparisons of the same category of axons in different nerve sections observed using SEM	63
Table 4.23: Mean diameter of total axons comparisons between nerve sections in the same animal observed using SEM	65
Table 4.24: Diameter comparisons of axons in the same nerve section observed from LM and SEM	66

## 1. INTRODUCTION

A number of techniques have been developed to repair damaged or dissected peripheral nerves. They include end-to-end suturing, fascicular suturing, nerve grafts, and nerve bridges. The choice of techniques depends upon the clinical situation and the surgeon's preference.

The end-to-end and the fascicular suture repair techniques are suitable for the nerve defect or injury which does not extend more than several millimeters. However, both of the techniques have their own disadvantages. In the end-to-end suturing technique, even though the outermost (epineural) layer of the dissected nerve ends is sutured together, poor alignment of fascicles and ingrowth of scar tissue into the nerve junction will result in unsatisfactory nerve function recovery (Marshall et al., 1989). In the fascicular suturing technique, a more precise alignment of fascicles is expected; however, the increased trauma to the perineurial and the intrafascicular tissue caused by the sutures will retard the nerve regeneration.

If the nerve injury is extensive and more than ten millimeters, then a nerve graft or a nerve bridge is preferred. It is difficult to acquire donor nerves for grafting. Thus, considerable research has been conducted on peripheral nerve repair using the nerve bridge technique (Jenq and Coggeshall, 1984, 1985, 1986, 1987; Seckel et al., 1984; Satou et al., 1986; Le Beau et al., 1988; Gibson and Daniloff, 1989). Most of this research has emphasized the use of single-lumen nerve guides of synthetic or biological origin. The multiple-lumen nerve guide in the *in vivo* repair of rat sciatic

nerve described by Daniel (1991) was the first attempt to develop a multiple-lumen nerve cuff to bridge a gap for peripheral nerve repair. The multiple-lumen repair cuff provides orientation, mechanical support, and guidance for the outgrowing Schwann cells and regenerating axons.

Regeneration and degeneration of nerve fibers and connective tissues after injury or severance of a peripheral nerve have been extensively studied using light (LM) and electron microscopy (EM) (Mira, 1979; Rosen et al., 1983, 1992; Jenq and Coggeshall, 1984, 1985, 1986, 1987; Espejo and Alvarez, 1986; Le Beau et al., 1988; Daniel, 1991). Scanning electron microscope (SEM) is an additional tool for study of regenerated nerves because of the ability to view large portions of tissue using an improvement of depth of field and resolution for a wide range of magnifications. Many SEM studies emphasize the surface morphology of regenerated nerve fibers after dissection or enzymatic digestion of the surrounding tissue (Gershenbaum and Roisen, 1978; Orgel and Huser, 1980; Miyakawa et al., 1981; Mathur et al., 1983; Kumagai et al., 1990; Tohyama and Kumagai, 1992). Therefore, information about the nerve tissue may be lost because of the surrounding tissue damage caused by the dissection or by other treatments of the nerve specimen. To solve this problem, some authors have suggested using the silver staining technique commonly applied in light microscopy (Lewis, 1971; DeNee et al., 1974; Tayler et al., 1984; Von Langsdorff et al., 1990). The silver impregnation methods have a high and specific affinity for neurofilament proteins and can be used to clearly outline individual axons without damaging the tissue surrounding the nerve fibers.



The present study was performed using the scanning electron microscope to observe rat sciatic nerve that had regenerated through single-lumen silicone rubber repair tubes by using a silver impregnation stain for the axons. Also morphological data obtained from light microscopy was related to SEM observations for identical cross sections in order to provide a more detailed evaluation of the regenerative process.

## **2. LITERATURE REVIEW**

### **2.1 Background**

#### **2.1.1 The mammalian peripheral nervous system**

Peripheral nerves are composed of numerous nerve fibers collected into several fascicles (bundles) and covered with a connective tissue sheath, the epineurium. Each fascicle within the epineurium is surrounded by a perineurium consisting of an outer connective tissue layer and an inner layer of flattened epithelioid cells. Each nerve fiber and associated Schwann cell has its own slender connective tissue sheath, the endoneurium. The endoneurium components include fibroblasts, an occasional macrophage, and collagenous and reticular fibers.

Each axon can be classified as myelinated or unmyelinated, depending on whether or not it has a coating of myelin. The region of the exposed axon at the junction between Schwann cells is called the node of Ranvier. These nodes are located at discrete intervals along the whole length of the myelinated axon (Jenq et al., 1986). Figure 2.1 is a schematic representation of a mammalian peripheral nerve and its components (Marshall et al., 1989).

#### **2.1.2 Nerve degeneration**

After nerve damage or severance, nerve degeneration occurs immediately. Waller (1850) states that the portion of the nerve that has been severed and separated from the central trophic area degenerates.

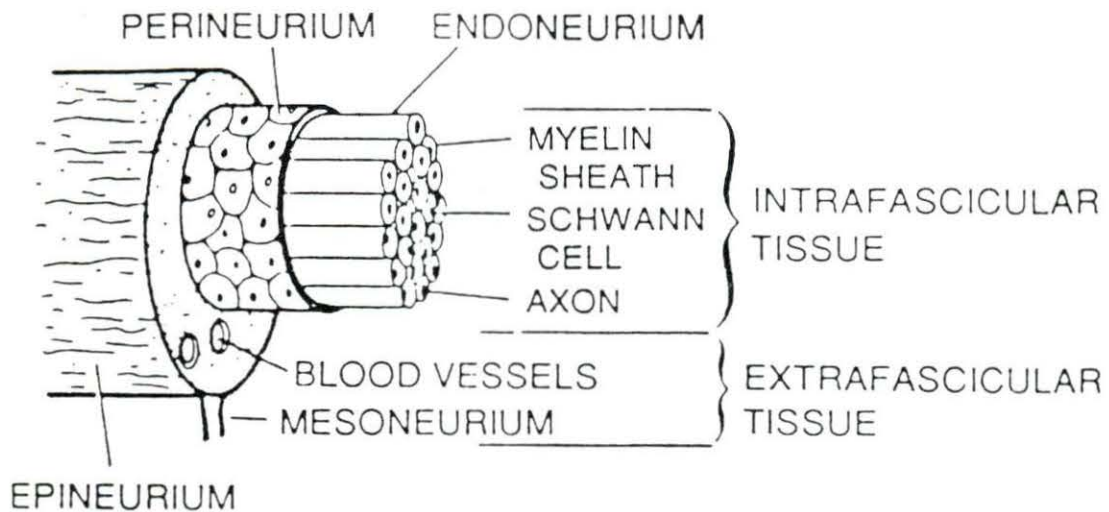


Figure 2.1: Schematic representation of the structure of a mammalian peripheral nerve (Marshall et al., 1989)

Regeneration begins from the undegenerated proximal stump. It remains connected to the trophic center. Many factors such as the site of the lesion, the age of the individual, the length of the nerve destroyed, the width of the severance gap, the alignment of the cut ends, and the amount of damage and hemorrhage in adjacent tissues affect the growth and development of the regenerating nerve (Swaim, 1987).

Hemorrhage and projection of a clot from the cut nerve ends occur immediately after nerve severance. Within 1 hour, there is marked swelling 0.5 to 1 cm on both sides of the point of transection because of the accumulation of blood serum, plasma, and acid mucopolysaccharides.

Degeneration that occurs in the proximal nerve stump is not as extensive as that in the distal stump. It is called traumatic degeneration. It does not extend beyond the second or third node of Ranvier from the injury site. However, damaged axon, myelin and sheath connective tissue due to extensive trauma may extend several centimeters on both sides of the severed nerve. The survival of the neurons is improved when the distance from the cell body to the point of axonal severance is relatively short. The entire distal stump begins to degenerate when the axons and their myelin start degenerating. However, for about 2 weeks, the axons at the proximal end of the distal stump tend to enlarge and get isolated from the rest of the distal stump. The remaining portions of the distal axons degenerate more rapidly. Axon and myelin degeneration become evident along the distal stump at 48 hours after nerve transection. The loss of the myelin layer around axons occurs and the degenerating myelin became homogeneous. The myelin becomes ovoid and elliptical surrounding axonal fragments. Neurofibrils in the axoplasm degenerate and disappear, while the optical density in the axoplasm increases and the axoplasm forms clumps. The connective tissue framework of the distal nerve stump disappears, while the degenerative products of axons and myelin are removed by the macrophages which appear from intra- and extraneural sources. Schwann cells are also known to participate in phagocytizing axonal and myelin breakdown products. The process of debris removal begins 21 days after injury and lasts five weeks. During the five week period, the distal nerve stump becomes less swollen, and the phagocytic activity slowly subsides. Neurilemmal sheaths realign in an orderly fashion, and endoneurial sheaths

shrink or disappear. If regenerating axons do not invade into the distal nerve stump, the distal stump becomes even more contracted and is replaced by connective tissue (Swaim, 1987).

Many investigators (O'Daly and Imaeda, 1967; Calabretta et al., 1973; Gershenbaum and Rosen, 1978; Ide et al., 1983; Tohyama et al., 1986) have observed the morphological alterations in the nerve fibers and connective tissues associated with Wallerian degeneration using light, transmission, and scanning electron microscopy. These studies provide a detailed account of the changes which occur during the degeneration of myelinated axons.

### **2.1.3. Nerve regeneration**

Nerve regeneration begins within the cell body and is similar in both motor and sensory nerves (Swaim, 1987). A considerable amount of energy that is expended by the cell body is required for the regeneration process. For approximately 10 to 20 days, the cell body becomes progressively larger owing to the chromatolysis. The cell body will not return to normal size until the nerve matures. During active regeneration, both RNA and DNA synthesis activity increase within the neuron. In addition, increased metabolic activity results in the increased enzymatic activity and incorporation of amino acids. The protein and organic material in the cell body increase by 50 to 100 times that compared to the normal soma. The alterations of the glial cells that surround the neuron also aid in supporting the increased metabolic activity in the neuronal soma.

The enlargement of the neuronal soma may peak early in the regeneration process and again as myoneural junctions are formed. The cell body may die if the injury is too close to it or, if it survives, the cell may not have enough metabolic capacity to support the axons that must be regenerated and axonal regeneration will not happen.

New protoplasm that is synthesized by the cell body migrates by axoplasmic flow from the neuronal soma down the axon. The axoplasmic flow has a slow and a fast component. The slow component (1mm/day) involves microperistalsis within the nerve trunk membrane, and the fast component (100mm/day) involves the microtubules. During the passage down the axon, a part of slowly transported proteins is used to replace catabolized enzymes in the membrane. Nevertheless, most of the proteins still reach the terminal segments of the axon. Microtubules provide the fast transport of axoplasm to supply the increased nutrient requirements and metabolic activity at the synaptic regions.

The changes that occur at and between the proximal and distal nerve stumps strongly influence the regeneration of a severed nerve. Proliferation of epineurial and endoneurial connective tissue, Schwann cells, and capillaries, which control the regeneration of axons at the proximal and distal nerve stumps occur within 1 to 3 days after injury. These tissues infiltrate the injury site and migrate toward each other and form a bridge and capillary bed between the stumps to make it easier for the regenerating axons to grow to the distal nerve stump.

The increased metabolic activity of the neuronal soma occurs 4 to 20 days after injury. It results in the sprouting of axons from the proximal stump.

Different types of injury result in different locations for the start of sprouting or budding of the regenerating axons. Budding begins at 1 to 3 cm proximal to the point of severance in the case of wide-spread traumatic injuries; however, this budding begins a few millimeters retrograde to the last node of Ranvier with a sharply localized injury.

Schwann cells of the proximal and distal nerve stumps probably play the most important role in axonal regeneration. As Schwann cells proliferate, they form longitudinally oriented bands of Büngner, which are continuous with the persisting Schwann tubes in the nerve stump (Allt, 1976; Spencer, 1977). The Schwann cells of each stump migrate toward each other and join. Because the Schwann cells of the proximal stump slightly precede those of the distal stump, they can be regarded as a guide for the regenerating axons. The rate of axonal regeneration at the marginal zone of realignment progresses about 0.25 mm/day. Beyond this point, regeneration occurs at the rate of 1 to 4 mm/day. Although 3 to 4 mm/day rate of regeneration for axonal tips occurs, the rate of functional return is only 1 to 2 mm/day. The axonal regeneration rate changes during the course of regeneration in a single nerve, with lag periods at the beginning and end of regeneration. The state of the motor end plate and the condition of health of the muscle fibers also influence the success of axonal regeneration. Thus, physical therapy and care of muscles and skin are important for successful peripheral nerve regeneration (Swaim, 1987).

Histologic changes of regenerated nerves associated with chronic compression when using repair cuffs have been studied (Mackinnon et al., 1985; O'Brien et al., 1987). They observed a marked increase in the amount

of blood vessel, perineurial and epineurial tissue and a decrease in the amount of neural elements. In addition, dramatic increases in fibrous tissue and an absence of normal fascicular patterns were seen in the regenerated nerves (Mathur et al., 1983; Gibson and Daniloff, 1989). A smaller mean axon diameter and a larger number of regenerated axons in the repaired nerves as compared to the normal control were also reported (Rosen et al., 1983, 1989; Henry et al., 1985).

## **2.2. Repair techniques**

Different types of injury and the gap length require different methods of nerve repair. For gap lengths less than 10 mm, the end-to-end anastomosis is optimal. However, for gap lengths larger than 10 mm, a graft is preferred. The autograft is the best option to repair injury nerves because it will not cause severe tissue reaction during the implantation period. Nevertheless, disadvantages of the autograft are the difficulty of acquiring a donor nerve for grafting and the inevitable risks of surgery at another site. To solve these problems, artificial nerve cuffs or guide tubes have been regarded as an alternative in the repair of injured nerves. Compared with nerve grafting, the implantation of nerve cuffs has resulted in good nerve regeneration.

Previous work in developing the artificial nerve cuffs and the materials used to fabricate them is described below.

In 1983, Mathur et al. used a polyglycolic acid tube (Davis & Geck) to bridge a 1cm sciatic nerve gap in New Zealand rabbits. After eight months, they found that nerves regenerated across the 1 cm gap through the



polyglycolic acid conduit and the regrowth of myelinated axons grouped into "mini-fascicles" containing increased connective tissue.

Seckel et al. (1984) used biodegradable nerve guides made of DL-lactic acid (internal diameter=2 mm, wall thickness=250  $\mu$ m) to bridge 5 mm and 10 mm gaps in adult Sprague-Dawley rats. Three months after repair, they observed the sciatic nerve of the adult rat successfully regenerated across the 5 mm gap through the biodegradable nerve guides, but across the 10 mm gap. They also found nerve regeneration in the biodegradable nerve guides did not elicit an evident immune response.

Satou et al. (1986) used a silicone tube filled with a small amount of collagen gel (Cell Matrix II) to study axon regeneration across a 5 mm gap in the rat sciatic nerve and compared it with the control side in which the gap space in the tube was left empty. They found more rapid growth of sprouting axons toward the distal stump in the collagen gel filled tube as compared to the control side. In addition, the proliferation of both fibroblasts and larger Schwann cells was inhibited. They concluded that appropriate exogenous fine material such as a collagen matrix can accelerate the regeneration of nerves in the silicone tube.

Valentini et al. (1987) used semipermeable polyvinyl-chloride acrylic copolymer guide tubes (wall thickness=0.15 mm) filled with collagen (type I or type II) or laminin gel to repair 4 mm mice sciatic nerve gaps. After 12 weeks repair, they found fewer myelinated axons in the collagen gel filled tubes as compared to the control saline filled tubes. They concluded that the addition of growth-promoting substrates such as the collagen and laminin gels used in the present case can not improve nerve regeneration.

In 1989, Gibson and Daniloff used a silicone tube (Silastic, Dow Corning, 8mm in length) to bridge a gap of 5 mm in adult female Sprague-Dawley rats and compared it with a nerve allograft. Electromyography was used to provide an objective assessment of functional nerve regeneration. At 90 days post-implantation, the nerve graft group had superior conduction velocity times as compared to the silicone implant group. They suggested that if a nerve cuff is used in repair of a transected nerve, it should be large enough to accommodate nerve enlargement or should be removed after the regenerating axons have bridged the transection site.

In 1992, Rosen et al. used a synthetic biodegradable conduit made of glycolide trimethylene carbonate (10 mm long) filled with a liquid collagen (Collagen [C3511]) to bridge gaps of 5 mm in adult Sprague-Dawley rat peroneal nerves. They compared the results for this case with sutured autografts. These rats were evaluated after 6 to 9 months of repair. They observed that there is negligible inflammatory response to the collagen matrix. Regenerated axon diameters were equal in the synthetic biodegradable conduit groups as compared to the sutured autograft groups.

### **2.3. Characteristics of the silicone rubber cuffs**

After eliminating the impurities, silicone rubbers can be produced with average molecular weights into the millions. The methyl side groups of the polymer can be replaced by a vinyl or phenyl side groups to form methyl/vinyl, methyl/phenyl, or methyl/vinyl/phenyl copolymers, but the methyl side groups are generally predominant.

Cross-linking (vulcanization) is the process by which the polymer is turned into the three dimensional structure of a rubber with all its associated properties (Van Noort and Black, 1981). This process is initiated by a catalyst which in the case of heat vulcanizing silicone rubber is a dichlorobenzoyl peroxide (DBP). DBP will break down to form free radicals and release carbon dioxide while heated over 60° C.

The dichlorophenyl radicals which have the properties of strong dehydration and oxidization can activate the methyl and vinyl chains by a radical transfer mechanism. Cross links then can be established by these activated vinyl and methyl groups. This reaction can take place in many ways. In general, methyl-methyl and methyl-vinyl interactions are the two most commonly used (Braley, 1970).

#### **2.4. Silver staining of nerve tissue**

Silver staining is commonly used in analyzing the axon features because of its ability to aid in distinguishing axons from the unstained surrounding tissue. The Bodian's stain used in the present study is one of the most reliable. Neurofilament proteins in the normal axons have a strong and specific affinity for Bodian's silver. However, immature axons or fine cell elements with few neurofilament proteins will not be stained by the Bodian's method (Katz and Watson, 1985). The roles of the free silver ions and albumin carrier in the staining process remain unknown; however, a specific amino acid sequence in the neurofilament proteins may act as a determinant of binding the neurofilament proteins with the silver (Phillips et al., 1983).

Even though the exact reactions responsible for the selective affinity of Bodian's stain for neurofilament proteins remain to be discovered, the details of the chemical reactions that occur during the silver staining are well known.

In the early stage of the staining, impregnation by silver results in the formation of silver nuclei in both axons and myelin. However, after exposure of the section to the action of reducing agents (e.g. formalin, pyrogallol, or hydroquinone), the impregnation of axons increases without the myelin being affected. The phenomena can be explained by assuming that the axons contain more reducing groups than myelin (Wolman, 1955). After sections are impregnated by silver solutions, the sections can be treated with gold chloride to intensify the contrast between the more strongly stained areas and the less intensely impregnated sites.

## **2.5. Scanning electron microscopy**

SEM provides three-dimensional information which can aid in the interpretation of the two-dimensional ultrastructural changes seen with the light or the transmission electron microscope (Gershenbaum and Roisen, 1978). The powerful capability of the scanning electron microscope for the study of nerve tissue is due to the interactions between the primary beam electrons and the specimen atoms. These interactions may be placed into two groups:

(1). Elastic events. A primary beam electron comes close to a specimen atom nucleus or outer shell electron and rebounds with no significant energy

loss. These kinds of scattered electrons are referred to as backscatter electrons.

(2). Inelastic collisions. A primary beam electron collides with a specimen atom and results in a loss of energy from that atom, leading to the generation of secondary electrons, Auger electrons, characteristic and continuum X-rays.

The electrons are collected by a detector system (a different system for each variety) and converted to an electronic signal which is displayed on a cathode ray tube. The scanning of the SEM beam is synchronized with the scanning of the electron beam of the cathode ray tube, thus producing a representation of the area scanned on the CRT. Secondary electrons and/or backscatter electrons are frequently used in providing nerve tissue microstructural information.

### **2.5.1. Secondary electrons**

The low energy electrons emitted from a sample with an energy less than 50 eV are usually regarded as the secondary electrons. The escape depth of secondary electrons represents only a small fraction of the primary electron range. The secondary emission images provide information about the surface topography.

### **2.5.2. Backscatter electrons**

A significant fraction of the beam electrons will escape after striking a target. The reemergent beam electrons are known as backscatter electrons. The yield of backscatter electrons is dependent on differences in the

specimen's mean atomic number. The higher the atomic number regions, the more backscattering of electrons. The backscatter electron signal can be used to derive useful information about the relative difference in average atomic number of regions of a specimen. In this way, silver-impregnated nerve fibers (atomic number=47) can be easily distinguished from the unstained surrounding tissue (atomic number approximately=6) using a SEM equipped with a backscatter electron detector (Taylor et al., 1984; Von Langsdorff et al., 1990).

### 3. MATERIALS AND METHODS

#### 3.1 Samples

A new type of nerve repair cuff, the multiple-lumen silicone rubber nerve cuff, was described by Daniel (1991). Observations made from the multiple-lumen cuff nerve repairs were compared with results obtained from normal controls, end-to-end nerve repairs, and single-lumen silicone rubber cuff repairs. Sixteen Sprague-Dawley adult male rats were used by Daniel for single-lumen silicone rubber cuff studies. The current project is an extension of these studies with an emphasis on single lumen nerve cuff repair. These nerve specimens had been sectioned at 1.5 to 2.5  $\mu\text{m}$  thick, silver stained, toned with gold chloride, and mounted on microscopic slides for light microscopic observations. The slides were obtained from proximal, middle, and distal sciatic nerve sections obtained at 8, 12, 16, and 24 weeks after implantation.

The present study represents a substantial increase in the portions of the nerve section areas studied by light microscopy (LM) so that statistical tests could be performed to establish size relationships for axons from the proximal, middle, and distal sections. In addition, a new approach has been taken to more fully characterize microstructural features of these samples. As the light microscope samples were stained with silver for visualization, the same samples offered a way to examine details of the axons of these nerve sections at higher magnifications using electron backscatter imaging, as well as to expand certain light microscope studies.

### 3.2 Light microscopy and scanning electron microscopy

Micrographs of a normal control and the proximal, middle, and distal cross-sections of the regenerated nerves from the single lumen silicone rubber cuff studies were taken by light and scanning electron microscopy. The light micrographs were taken at 160X with a Dialux 20 (Leitz) light microscope. The type of film used was TP135-36 Kodak Technical Pan film.

To examine the specimens under scanning electron microscopy, it was necessary to take the glass cover slip off the sample mounted on the glass slide. This was accomplished by placing selected slides in xylene. After five days, the xylene dissolved the adhesive that held the glass cover slip onto the top of the thin section. The cover slip was then taken off using tweezers. The thin section remained attached to the underlying glass slide. The samples were then stored in a desiccator. The specimens were coated with a 150Å thin film of gold using a sputtering device (sample sputter coating unit E5100, Polaron Instruments Inc.) operated for one minute at 2.2 keV and 20 mA ion current. To avoid specimen charging problems in the SEM, the edge of the glass slide was covered with a conductive adhesive (a mixture of colloidal graphite and isopropanol, Energy Beam Sciences, MA) and grounded to the sample stage. The specimens were then studied using a JEOL-840A scanning electron microscope equipped with a solid state backscatter electron detector. Secondary electron images were obtained using an accelerating voltage of 15 kV, an aperture size of 70 μm, a 23 mm working distance, and a probe current of 0.3 nA. Backscatter electron images were also obtained. These images were taken at an accelerating



voltage of 15 kV, an aperture size of 70  $\mu\text{m}$ , and a probe current of 0.02 to 0.3 nA. In addition, a smaller working distance (7 mm or 13 mm) was used to improve the resolution and signal strength for the electron backscatter images. The scanning electron micrographs were obtained using Type 55 positive/negative Polaroid film.

### **3.3 Quantitative evaluations**

#### **3.3.1 Quantitative studies**

The proximal, middle, and distal cross-sections for each animal were used for axon size and distribution studies. Selected sections were photographed using the light microscope and then enlarged. The magnification of the enlarged micrographs was evaluated as follows. First, two locations on a feature in a micrograph were selected and the distance between them was measured. The two spots were also located on the negative that was used to make the enlarged micrograph and the distance between them was measured at 100 magnification using a Zeiss light microscope equipped with a calibrated Filar micrometer eyepiece (Bausch & Lomb). The magnification of the enlarged micrograph was then obtained by dividing the distance value measured from the enlargement by that obtained from the microscope and multiplying the result by the true magnification of the negative which was obtained by direct measurement of the same feature distances using LM. Ten successive measurements of the magnifications for different locations were done and the mean of the ten measurements was taken as the true magnification of the enlarged micrograph (enlargement

range was 360 to 380X). Micrographs of the nerve sections were also obtained using a scanning electron microscope (SEM). All the SEM micrographs used for quantitative evaluations were at 1000 magnification. This permitted axon diameters to be specified to  $\pm 0.2 \mu\text{m}$ . The sample identifications are listed in Table 3.1 for the LM and SEM study.

Table 3.1: Implant period, type of repair, animal number, nerve section, and slide number for sections used in the present LM and SEM study

Implant Period & Type of Repair	Animal Number	Nerve Section	Slide Number
8 Weeks Single-Lumen	#41	Proximal	91R632A
		Middle	91R632C
		Distal	91R632B
12 Weeks Single-Lumen	#43	Proximal	91R643A
		Middle	91R643C
		Distal	91R643B
16 Weeks Single-Lumen	#16	Proximal	91R726A
		Middle	91R726C
		Distal	91R726B
24 Weeks Single-Lumen	#5	Proximal	91R716A
		Middle	91R716C
		Distal	91R716B
	#6	Proximal	91R717A
		Middle	91R717C
		Distal	91R717B
	#47	Proximal	91R732A
		Middle	91R732C
		Distal	91R732B
	#48	Proximal	91R733A
		Middle	91R733C
		Distal	91R733B
24 Weeks Normal Control	#9	Middle	91R720

Morphometric parameters of the examined nerves such as reference area, axon core diameters, axon counts, major and minor maximum diameter ratio, nerve area, axons per unit area, and percentage of nerve examined were obtained from LM and SEM. Details of the measurement methods are described in the following seven sections.

#### **3.3.1.1 Reference area**

To compare the axon regeneration among experimental and control specimens a grid overlay was used. The reference area for the section was then determined by summing the actual area values for all the squares of the grid. Axon counts and axon diameters were then measured for these grid regions. Area measurements are reported to the nearest 500  $\mu\text{m}$ .

#### **3.3.1.2 Axon counts**

All of the axons in one square of the magnified photograph of the section were counted and marked off. When all the axons in one square of the section had been measured in this way, those of a second square were measured, and so on until all squares had been included. Axon counts were made of the axons in these squares, and the total number of axons in the section was then estimated from the axon counts and the total number of squares occupied by the nerve cross section.

#### **3.3.1.3 Axon core diameter and average axon diameter**

Two measurements were made of the diameter of each axon, one along the largest diameter and the other for the longest dimension

perpendicular to the first. The mean of the two measurements was then taken as the axon core diameter. The average axon diameter of the nerve section was obtained by summing these diameter values for all of the axons of the reference area and then dividing the result by the axon counts.

#### **3.3.1.4 Diameter ratio and mean diameter ratio**

The two axon diameter measurements described above were used to determine the diameter ratio. This quantity was obtained by dividing the largest axon diameter by the other obtained at right angles to the first. The mean diameter ratio for a section was then obtained by summing these ratio values for all of the axons and dividing the result by the axon counts.

#### **3.3.1.5 Axons per unit area**

This quantity was obtained by dividing the axon counts by the reference area.

#### **3.3.1.6 Nerve area**

Grid area measurements were also used to determine the total area of a nerve.

#### **3.3.1.7 Percentage of nerve examined**

This quantity was determined by dividing the reference area by the nerve area. This was then expressed as the percentage examined.

### **3.3.2 Preparation of fiber diameter histograms**

The fiber diameter histograms of the controls and the single-lumen nerve repairs for the four time periods were plotted as percentage of total axons measured versus the axon core diameter. The axon distributions were determined for the proximal, the middle, and the distal sections for each animal. Small axons less than 1  $\mu\text{m}$  in diameter were not represented in the histograms. Also, the total percentage of axons within  $\pm 1 \mu\text{m}$  of the mean axon diameter in each section was tabulated.

## **3.4 Statistical Methods**

Analysis of variance was performed on the quantitative data obtained from light and scanning electron microscopy. Tukey's test (Byrkit, 1987), which is capable of multiple comparisons between group means with different numbers of observations, was used to determine whether or not the differences among the mean axon diameters obtained from measurements for each of the sections in repaired nerves were significant, and whether or not the mean axon diameter differences were significant for each section in repaired nerves compared to the normal control. For each section, the mean axon diameters obtained from both LM and SEM were also compared. The statistical analysis was performed using the Statistical Analysis System (Cary, NC) version 6.06.

## 4. RESULTS

### 4.1 Microstructure

The normal control sections and the proximal, middle, and distal cross-sections of the regenerated nerves (8, 12, 16, and 24 week periods) observed using LM have been described by Daniel (1991). In the present study, these nerve specimens were also observed using the SEM.

The secondary electron image of an undamaged normal control is shown in Figure 4.1. The surfaces of axons were covered with the adhesive (Acrytol) remaining after removal of the glass cover slip which had been on top of this surface. The axons were not easy to discriminate in this type of image. However, in the backscatter electron images, the backscatter electrons passed through the thin layer of residual adhesive and revealed the underlying silver-stained axons as bright irregular-shaped closely packed structures (Figure 4.2). For this reason, backscatter electron images were the primary type analyzed in the study.

From the backscatter electron images, two general shapes of axons were seen: (1) approximately circular axons (cross section fully stained) which were termed category I axons and (2) elliptical or arcuate shaped axons or stained rim shaped features which were termed category II axons. These features are not seen clearly in LM images. Examples are shown in the SEM image of Figure 4.3.

Also, nerve specimens contained small particulates of silver approximately 1  $\mu\text{m}$  or less in diameter (Figure 4.4). However, these

Figure 4.1: Secondary electron micrograph of a cross-section of the right sciatic nerve at the mid-thigh level from a normal control, (animal #9, 24 weeks). Bodian stain. Scale bar=10  $\mu\text{m}$

Figure 4.2: Backscatter electron micrograph of the identical field as Figure 4.1. Axons are the bright features surrounded by myelin sheaths. Bodian stain. Scale bar=10  $\mu\text{m}$

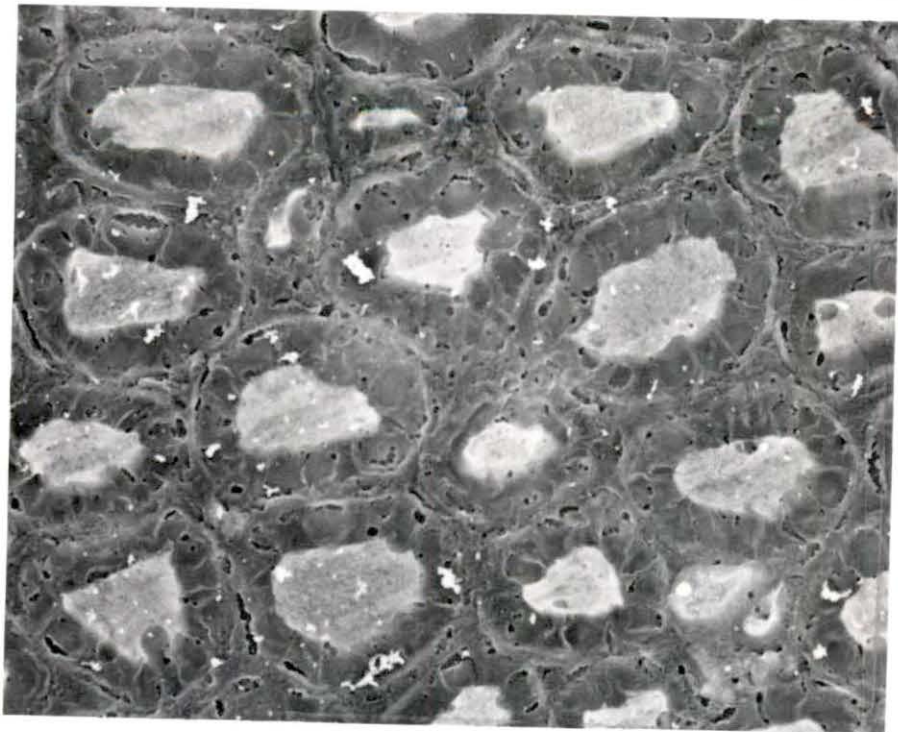
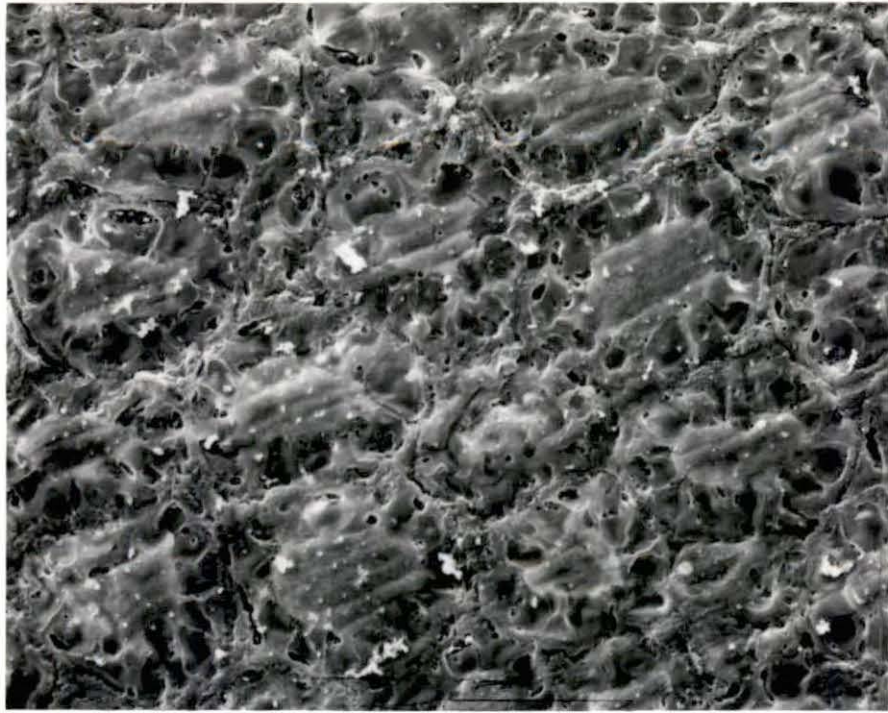
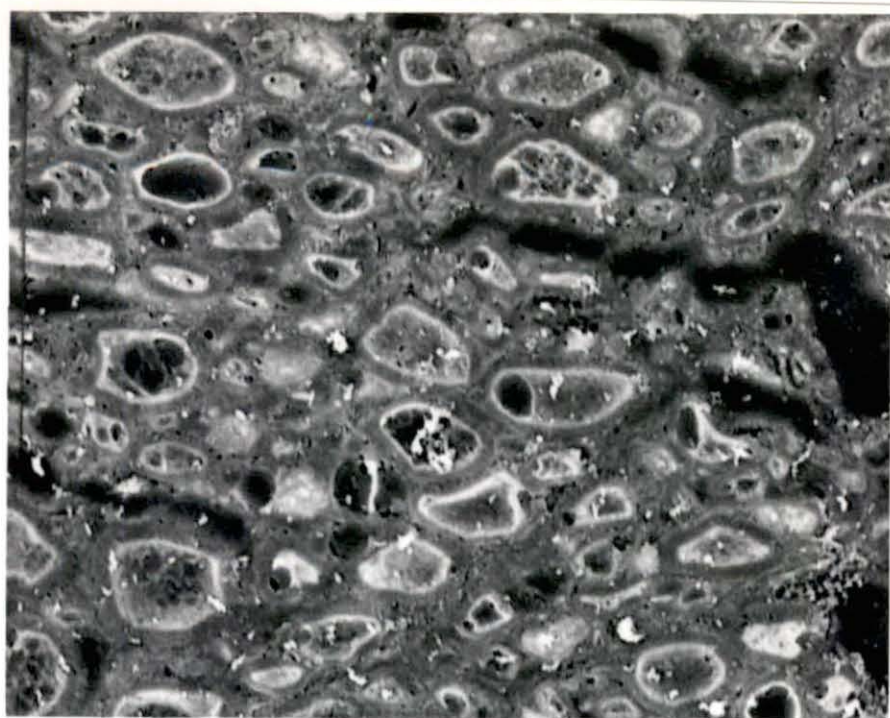




Figure 4.3: Backscatter electron image of a single-lumen cuff nerve section, (animal #48, middle section, 24 weeks). Category I and category II axons are in the field of view. Bodian stain. Scale bar=10  $\mu\text{m}$

Figure 4.4: Backscatter electron image showing silver grains on the surface for a region of a single-lumen cuff nerve section, (animal #41, middle section, 24 weeks). Some regions of nerve sections were heavily covered with these features whereas even on the same section there were regions with relatively few particles of this type on the surface. Bodian stain. Scale bar=2  $\mu\text{m}$



particles did not seriously interfere with the observations of the axons in the nerve cross sections.

#### **4.1.1 Control**

Figure 4.2 presents a cross sectional view of the sciatic nerve from a normal control rat. The axons of category I and category II were seen. The two types of axons varied in diameter and were closely packed in the nerve bundles. Some blood vessels were seen among the axons.

#### **4.1.2 Proximal section**

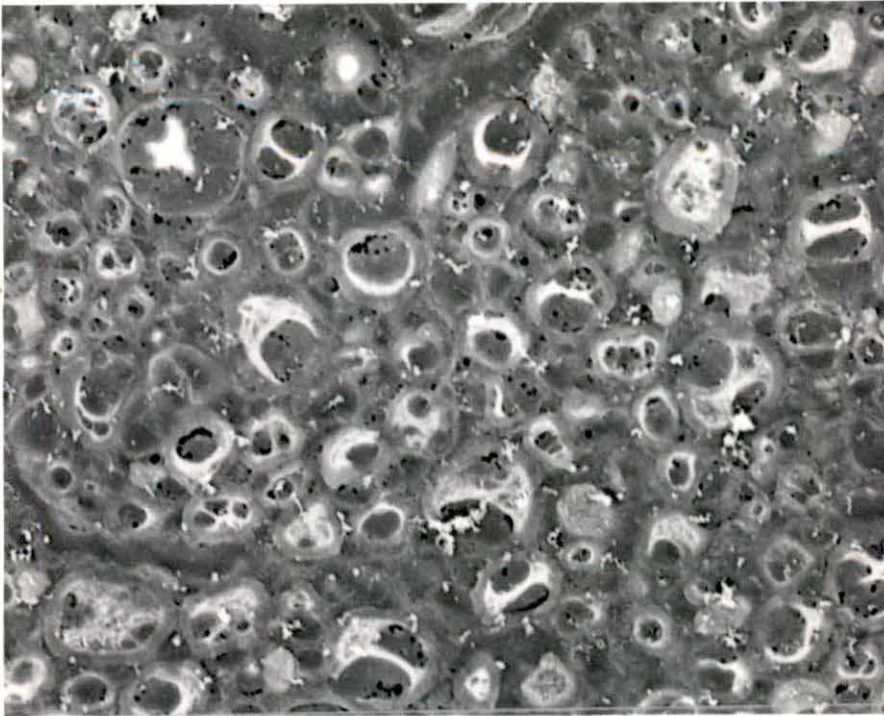
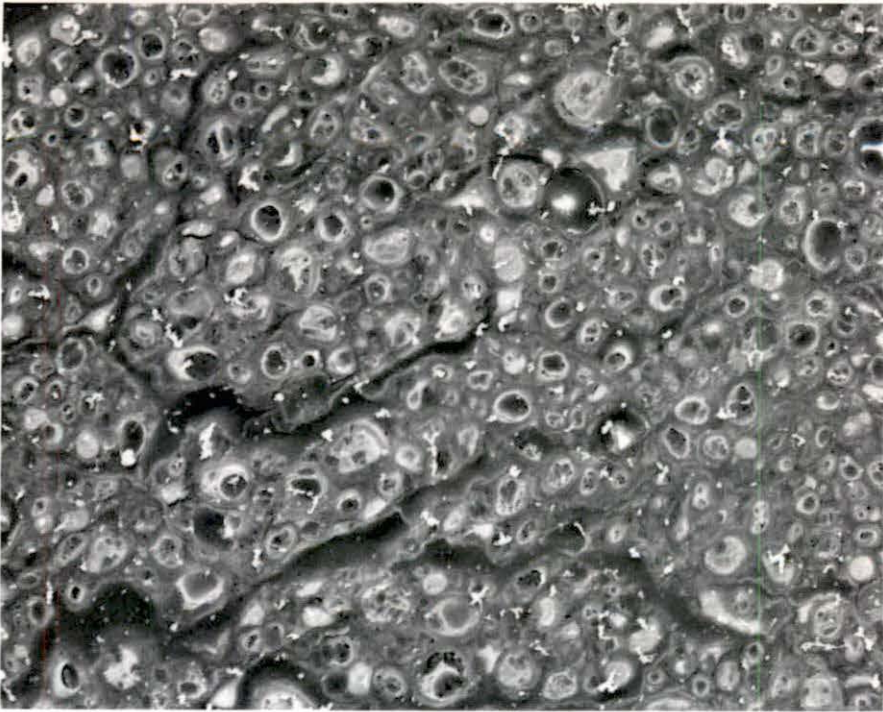
The structure changed dramatically at the proximal sites for all four time periods. As compared with the normal control, the differences in numbers and sizes of the category I and the category II axons were significant and a relatively larger fraction of the regenerated nerve cross sectional area was covered with connective tissue. Regenerated axons grouped to form microfascicles and axons in the microfascicles were separated by the connective tissue (Figure 4.5).

#### **4.1.3 Middle section**

The structure of the middle sections was similar to that seen in the proximal sections as described above, except for the numbers and sizes of the regenerated axons (Figure 4.6).

Figure 4.5: Backscatter electron image of a single-lumen cuff nerve section, (animal #6, proximal section, 24 weeks). Microfascicles are apparent. Category I and category II axons are seen. Bodian stain. Scale bar=10  $\mu\text{m}$

Figure 4.6: Backscatter electron image of a single-lumen cuff nerve section, (animal #6, middle section, 24 weeks). Category I and category II axons are seen. Bodian stain. Scale bar=10  $\mu\text{m}$



#### 4.1.4 Distal section

The structural differences were not significant at the distal section as compared to the proximal and middle sections (Figure 4.7).

### 4.2 Fiber diameter histograms

The fiber diameter histograms for the experimental and the control sections for the four time periods are shown in Appendix. They are designated LM or SEM analyses for the particular animals of Table 3.1.

Four low-resolution LM micrographs were too obscure to permit analyses of the regenerated axons. They included one from the proximal section of 8 weeks post-implantation nerve, two from the proximal and distal sections of 12 weeks post-implantation nerve, and one from the distal section of 16 weeks post-implantation nerve.

In backscatter electron micrographs, category I and category II axon size distributions were determined. In addition, the two types of axons were combined to obtain the total axon fiber diameter histograms for the various sections.

Moreover, distributions of percentage of axons within  $\pm 1 \mu\text{m}$  of the mean diameter for each nerve section observed using both LM and SEM are displayed in Table 4.1 through Table 4.4. Table 4.1 shows the distributions for the axons observed using LM. Table 4.2, Table 4.3, and Table 4.4 show the distributions respectively for the category I axons, the category II axons, and the total axons respectively using SEM.

Figure 4.7: Backscatter electron image of a single-lumen cuff nerve section, (animal #6, distal section, 24 weeks). Category I and category II axons are seen. Bodian stain. Scale bar=10  $\mu$ m

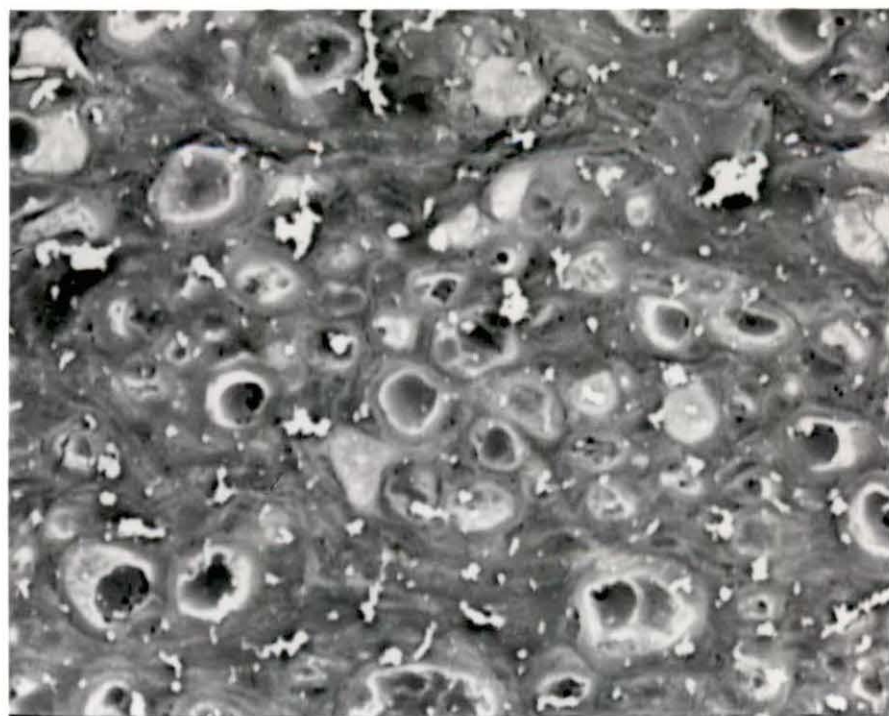




Table 4.1: Distributions of percentage of axons within  $\pm 1 \mu\text{m}$  of the mean diameter observed using LM

Implant Period, Type of Repair & Animal Number	Nerve Section	Percentage of Axons Within $\pm 1 \mu\text{m}$ of the Mean Diameter										
		Scale ( $\mu\text{m}$ )										
		1	1.5	2	2.5	3	3.5	4	4.5	5	5.5	6
24 Weeks, SL <sup>a</sup> #5	Proximal											77
	Middle						80					
	Distal					85						
#6	Proximal								71			
	Middle				84							
	Distal							68				
#47	Proximal									52		
	Middle						72					
	Distal								64			
#48	Proximal								64			
	Middle						82					
	Distal					65						
16 Weeks, SL #16	Proximal				84							
	Middle				92							
	Distal											
12 Weeks, SL #43	Proximal											
	Middle							78				
	Distal											
8 Weeks, SL #41	Proximal											
	Middle				89							
	Distal						81					
24 Weeks, NC <sup>c</sup> #9	Middle											46

<sup>a</sup>SL=Single-lumen cuff.

<sup>b</sup>Not Available.

<sup>c</sup>NC=Normal Control.

Table 4.2: Distributions of percentage of category I axons within  $\pm 1 \mu\text{m}$  of the mean diameter observed using SEM

Implant Period, Type of Repair & Animal Number	Nerve Section	Percentage of Axons Within $\pm 1 \mu\text{m}$ of the Mean Diameter										
		Scale ( $\mu\text{m}$ )										
		1	1.5	2	2.5	3	3.5	4	4.5	5	5.5	6
24 Weeks, SL <sup>a</sup> #5	Proximal						70					
	Middle				88							
	Distal			85								
#6	Proximal					91						
	Middle					79						
	Distal						83					
#47	Proximal									51		
	Middle						83					
	Distal							82				
#48	Proximal						81					
	Middle						70					
	Distal						77					
16 Weeks, SL #16	Proximal					83						
	Middle			92								
	Distal							67				
12 Weeks, SL #43	Proximal					86						
	Middle					78						
	Distal							75				
8 Weeks, SL #41	Proximal					71						
	Middle					80						
	Distal					85						
24 Weeks, NC <sup>b</sup> #9	Middle								47			

<sup>a</sup>SL=Single-lumen cuff.

<sup>b</sup>NC=Normal Control.

Table 4.3: Distributions of percentage of category II axons within  $\pm 1 \mu\text{m}$  of the mean diameter observed using SEM

Implant Period, Type of Repair & Animal Number	Nerve Section	Percentage of Axons Within $\pm 1 \mu\text{m}$ of the Mean Diameter										
		Scale ( $\mu\text{m}$ )										
		1	1.5	2	2.5	3	3.5	4	4.5	5	5.5	6
24 Weeks, SL <sup>a</sup> #5	Proximal					71						
	Middle			87								
	Distal				85							
#6	Proximal						74					
	Middle						79					
	Distal						72					
#47	Proximal										59	
	Middle						72					
	Distal								68			
#48	Proximal						76					
	Middle						74					
	Distal							75				
16 Weeks, SL #16	Proximal					74						
	Middle					89						
	Distal								62			
12 Weeks, SL #43	Proximal						74					
	Middle						82					
	Distal								70			
8 Weeks, SL #41	Proximal						76					
	Middle					83						
	Distal						77					
24 Weeks, NC <sup>b</sup> #9	Middle									61		

<sup>a</sup>SL=Single-lumen cuff.

<sup>b</sup>NC=Normal Control.

Table 4.4: Distributions of percentage of total axons within  $\pm 1 \mu\text{m}$  of the mean diameter observed using SEM

Implant Period, Type of Repair & Animal Number	Nerve Section	Percentage of Axons Within $\pm 1 \mu\text{m}$ of the Mean Diameter										
		Scale ( $\mu\text{m}$ )										
		1	1.5	2	2.5	3	3.5	4	4.5	5	5.5	6
24 Weeks, SL <sup>a</sup> #5	Proximal						61					
	Middle				87							
	Distal				83							
#6	Proximal					81						
	Middle						78					
	Distal						76					
#47	Proximal										53	
	Middle						75					
	Distal								66			
#48	Proximal						78					
	Middle						72					
	Distal							70				
16 Weeks, SL #16	Proximal					76						
	Middle				88							
	Distal								64			
12 Weeks, SL #43	Proximal					80						
	Middle						77					
	Distal							73				
8 Weeks, SL #41	Proximal					71						
	Middle				81							
	Distal				80							
24 Weeks, NC <sup>b</sup> #9	Middle									50		

<sup>a</sup>SL=Single-lumen cuff.

<sup>b</sup>NC=Normal Control.

## **4.2.1 Fiber diameter histograms observed using LM**

### **4.2.1.1 Eight Weeks**

The fiber diameter histograms were generated for the single lumen nerve cuff experiment for one animal. More than 80% of the middle and the distal distributions were at diameters within  $\pm 1 \mu\text{m}$  of their mean diameters. A larger peak occurred at  $3.5 \mu\text{m}$  in the distal distributions as compared to that occurring at  $2.5 \mu\text{m}$  in the middle distributions.

### **4.2.1.2 Twelve Weeks**

The fiber diameter histograms were generated for the single lumen nerve cuff experiment for one animal. The middle distribution in the group was between  $1.5$  to  $8 \mu\text{m}$  and exhibited a skewed distribution, with a peak occurring at  $3.0 \mu\text{m}$ . Approximately 78% of the middle distributions were within  $\pm 1 \mu\text{m}$  of the mean diameter.

### **4.2.1.3 Sixteen Weeks**

The fiber diameter histograms were generated for the single lumen nerve cuff experiment for one animal. More than 90% of the proximal and middle distributions were smaller than  $4.5 \mu\text{m}$  and both of the distributions had a peak occurring at  $2.5 \mu\text{m}$ . More than 80% of the proximal and the middle distributions were at diameters within  $\pm 1 \mu\text{m}$  of their mean diameters.

#### **4.2.1.4 Twenty-Four Weeks**

The fiber diameter histograms were generated for four single lumen nerve cuff experimental animals and for one normal control animal. In the cuff experiments, the proximal distributions for all the four animals were located at somewhat larger diameters, as compared to the middle and distal distributions. More than 60% of the distributions at the three nerve sections in each animal were within  $\pm 1 \mu\text{m}$  of their mean diameters except in the proximal section of animal #47. The normal control animal data showed a bimodal distribution with peaks occurring at 4.0 and 5.0  $\mu\text{m}$  and more than 80% of the axons were located between 2.5 and 8.5  $\mu\text{m}$ . Only 46% of the axons were within  $\pm 1 \mu\text{m}$  of the mean diameter.

### **4.2.2 Fiber diameter histograms observed using SEM**

#### **4.2.2.1 Eight Weeks**

The fiber diameter histograms were generated for the single lumen nerve cuff experiment for one animal. In the category I axon group, the distributions at the three sections showed skewed distributions toward smaller sizes, with most of the groupings occurring between 1.5 and 4.0  $\mu\text{m}$ . A larger peak (3.5  $\mu\text{m}$ ) was in the distal distributions in contrast to the middle and proximal distributions. In the category II axon group, approximately 90% of the distributions at all three sections were located between 2.0 and 5.0  $\mu\text{m}$ . In the total axon group, more than 95% of the distributions at the three sections were smaller than 5.5  $\mu\text{m}$ , with maximum axon numbers occurring between 2.5 and 3.5  $\mu\text{m}$ . For the three axon groups in each nerve section,

more than 70% of the axon distributions were within  $\pm 1 \mu\text{m}$  of their mean diameters.

#### **4.2.2.2 Twelve Weeks**

The fiber diameter histograms were generated for the single lumen nerve cuff experiment for one animal. In the category I axon group, the peak in the distal distributions were located at a larger diameter ( $3.5 \mu\text{m}$ ) as compared to the middle and proximal distributions. More than 50% of the proximal distribution occurred at the smaller diameters (between  $2.5$  and  $3 \mu\text{m}$ ), with the middle distributions located between the proximal and distal distributions. In the category II axon group, no diameters smaller than  $2.0 \mu\text{m}$  occurred in the middle and distal distributions. A larger peak was located at  $3.5 \mu\text{m}$  in the distal section in contrast to the proximal and middle sections. In the total axon group, the distal distributions were located at larger diameters (between  $3.5$  and  $4.5 \mu\text{m}$ ), as compared to the proximal and middle distributions. More than 70% of the distributions for the three axon groups in each nerve section were within  $\pm 1 \mu\text{m}$  of their mean diameters.

#### **4.2.2.3 Sixteen Weeks**

The fiber diameter histograms were generated for the single lumen nerve cuff experiment for one animal. The distal distributions in all groups were located at larger diameters between  $3.0$  and  $4.5 \mu\text{m}$ , as compared to the proximal and middle distributions. No diameters larger than  $5.5 \mu\text{m}$  occurred in all middle distributions. Approximately 60% to 90% of the

distributions for the three axon groups in each nerve section were within  $\pm 1$   $\mu\text{m}$  of their mean diameters.

#### **4.2.2.4 Twenty-Four Weeks**

The fiber diameter histograms were generated for four single lumen nerve cuff experimental animals and for one normal control animal. In the cuff experiments, the proximal distributions of the category I axon group were located between 2.0 and 9.5  $\mu\text{m}$  in animal #47 (a wide spread), and between 1.0 and 7.0  $\mu\text{m}$  in the three other animals. The proximal distributions of all the four animals were located at larger diameters between 3.0 and 4.5  $\mu\text{m}$  as compared to the middle and distal distributions. In the category II axon group, the distributions at the three sections showed skewed distributions toward the smaller sizes. A wide diameter distribution from 1.5 to 10.5  $\mu\text{m}$  also occurred in animal #47. In the total axon group, the proximal and distal distributions occurred at larger diameters (between 2.0 and 4.5  $\mu\text{m}$ ) and the middle distributions were located at the smaller diameters (between 2.0 to 3.0  $\mu\text{m}$ ). More than 60% of the distributions for the three axon groups in each of the three nerve sections were within  $\pm 1$   $\mu\text{m}$  of their mean diameters, except in the proximal section of animal #47.

In the normal control animal, a bimodal distribution with peaks occurring at 3.0 and 5.5  $\mu\text{m}$  occurred in the category I axon and in the total stained axon groups. Approximately 50% of diameter distributions in the category II axon group occurred at 5.0 and 5.5  $\mu\text{m}$ . Less than 60% of distributions for the category I axon and the total axon group were within  $\pm 1$   $\mu\text{m}$  of their mean diameters.



### 4.3 Quantitative results

The quantitative data were obtained from light and scanning electron micrographs. It should be noted that in the normal control animal, the quantitative data were obtained from sections taken from only one site in the sciatic nerve which was comparable to the middle of the repair site in the single-lumen cuff repaired nerves since the separation was only at one location. Four low-resolution LM micrographs as described before were not studied in the quantitative evaluations. In the SEM micrographs, the category I and the category II axons were used for the quantitative study. Moreover, the total axons which combined the two types of axons were also studied. The quantitative results are shown in Table 4.5 through Table 4.16. Table 4.5 to Table 4.8 list the axon counts, reference area, and axons per unit area observed using LM and SEM. Table 4.9 to Table 4.12 list the mean axon diameter, nerve area, and percentage of nerve observed using LM and SEM. Table 4.13 to Table 4.16 list the axon diameter ratio and estimated total number of axons in each nerve cross section observed using LM and SEM. The results in these tables are grouped according to the nerve sites examined and to the implantation periods. Means and standard deviations are also presented.

In addition to the comparisons described in the Statistical Methods, additional statistical comparisons were done for the SEM category I and category II axons. First, Tukey's test was used to determine whether or not the differences of the mean diameters obtained from the measurements for the two types of axons in each nerve section were significant and whether or

Table 4.5: Axon counts, reference area and axons per unit area observed using LM

Implant Period & Type of Repair	Animal Number	Axon Counts (#)			Reference Area ( $\mu\text{m}^2$ )			Axons per Unit Area (axons per $\mu\text{m}^2$ )		
		Prox	Mid	Dist	Prox	Mid	Dist	Prox	Mid	Dist
24 Weeks										
Single Lumen	#5	4110	5920	3528	277500	256000	152000	0.015	0.023	0.023
	#6	3768	4632	2360	271500	199500	137500	0.014	0.023	0.017
	#47	2800	4392	2124	274500	250000	168500	0.010	0.018	0.013
	#48	2176	3198	3507	185000	192000	190000	0.012	0.017	0.018
	Mean	3214	4536	2880	252000	224500	162000	0.013	0.020	0.018
	SD <sup>a</sup>	887	1116	743	45000	33500	22500	0.002	0.003	0.004
16 Weeks										
Single Lumen	#16	3924	3190	N/A <sup>b</sup>	191000	116000	N/A	0.021	0.028	N/A
12 Weeks										
Single Lumen	#43	N/A	4070	N/A	N/A	258500	N/A	N/A	0.016	N/A
8 Weeks										
Single Lumen	#41	N/A	3860	1862	N/A	140500	95500	N/A	0.027	0.020
24 Weeks										
Normal Control	#9	— <sup>c</sup>	2285	—	—	230500	—	—	0.010	—

<sup>a</sup>SD=Standard Deviation.

<sup>b</sup>Not Available.

<sup>c</sup>Not Applicable.

Table 4.6: Category I axon counts, reference area and category I axons per unit area observed using SEM

Implant Period & Type of Repair	Animal Number	Axon Counts (#)			Reference Area ( $\mu\text{m}^2$ )			Axons per Unit Area (axons per $\mu\text{m}^2$ )		
		Prox	Mid	Dist	Prox	Mid	Dist	Prox	Mid	Dist
24 Weeks										
Single Lumen	#5	105	94	199	10000	10000	10000	0.010	0.009	0.020
	#6	53	42	66	10000	10000	10000	0.005	0.004	0.007
	#47	61	46	64	10000	7000	10000	0.006	0.007	0.006
	#48	88	88	42	10000	10000	10000	0.009	0.009	0.004
	Mean	77	68	93	10000	9000	10000	0.008	0.007	0.009
	SD <sup>a</sup>	24	27	72	0	2000	0	0.002	0.002	0.007
16 Weeks										
Single Lumen	#16	88	106	57	7000	10000	10000	0.013	0.011	0.006
12 Weeks										
Single Lumen	#43	49	108	61	10000	9500	10000	0.005	0.011	0.006
8 Weeks										
Single Lumen	#41	114	125	79	10000	10000	10000	0.011	0.013	0.008
24 Weeks										
Normal Control	#9	— <sup>b</sup>	78	—	—	10000	—	—	0.008	—

<sup>a</sup>SD=Standard Deviation.

<sup>b</sup>Not Applicable.

Table 4.7: Category II axon counts, reference area and category II axons per unit area observed using SEM

Implant Period & Type of Repair	Animal Number	Axon Counts (#)			Reference Area ( $\mu\text{m}^2$ )			Axons per Unit Area (axons per $\mu\text{m}^2$ )		
		Prox	Mid	Dist	Prox	Mid	Dist	Prox	Mid	Dist
<b>24 Weeks</b>										
Single Lumen	#5	72	187	119	10000	10000	10000	0.007	0.019	0.012
	#6	164	196	107	10000	10000	10000	0.016	0.020	0.011
	#47	129	133	65	10000	7000	10000	0.013	0.019	0.007
	#48	100	102	70	10000	10000	10000	0.010	0.010	0.007
	Mean	116	155	90	10000	9000	10000	0.012	0.007	0.009
	SD <sup>a</sup>	39	45	27	0	2000	0	0.004	0.005	0.003
<b>16 Weeks</b>										
Single Lumen	#16	131	179	98	7000	10000	10000	0.019	0.018	0.010
<b>12 Weeks</b>										
Single Lumen	#43	153	132	70	10000	9500	10000	0.015	0.014	0.007
<b>8 Weeks</b>										
Single Lumen	#41	85	173	124	10000	10000	10000	0.009	0.017	0.012
<b>24 Weeks</b>										
Normal Control	#9	— <sup>b</sup>	23	—	—	10000	—	—	0.002	—

<sup>a</sup>SD=Standard Deviation.

<sup>b</sup>Not Applicable.

Table 4.8: Total axon counts, reference area and axons per unit area observed using SEM

Implant Period & Type of Repair	Animal Number	Axon Counts (#)			Reference Area ( $\mu\text{m}^2$ )			Axons per Unit Area (axons per $\mu\text{m}^2$ )		
		Prox	Mid	Dist	Prox	Mid	Dist	Prox	Mid	Dist
24 Weeks										
Single Lumen	#5	177	281	318	10000	10000	10000	0.018	0.028	0.032
	#6	217	238	173	10000	10000	10000	0.022	0.024	0.017
	#47	190	179	129	10000	7000	10000	0.019	0.026	0.013
	#48	188	190	112	10000	10000	10000	0.019	0.019	0.011
	Mean	193	222	183	10000	9000	10000	0.020	0.024	0.018
	SD <sup>a</sup>	17	47	94	0	2000	0	0.002	0.004	0.010
16 Weeks										
Single Lumen	#16	219	285	155	7000	10000	10000	0.031	0.029	0.016
12 Weeks										
Single Lumen	#43	202	240	131	10000	9500	10000	0.020	0.025	0.013
8 Weeks										
Single Lumen	#41	199	298	203	10000	10000	10000	0.020	0.030	0.020
24 Weeks										
Normal Control	#9	— <sup>b</sup>	101	—	—	10000	—	—	0.010	—

<sup>a</sup>SD=Standard Deviation.

<sup>b</sup>Not Applicable.

Table 4.9: Mean axon diameter, nerve area and percentage of nerve observed using LM

Implant Period & Type of Repair	Animal Number	Mean Axon Diameter ± Standard Deviation ( $\mu\text{m}$ )			Nerve Area ( $\mu\text{m}^2$ )			Percentage of Nerve Examined (%)		
		Prox	Mid	Dist	Prox	Mid	Dist	Prox	Mid	Dist
24 Weeks										
Single Lumen	#5	3.2±1.0	2.7±1.0	2.6±1.0	1180000	550000	380000	24	47	40
	#6	3.6±1.3	2.5±0.9	3.3±1.2	570000	510000	910000	48	39	15
	#47	4.6±1.7	3.5±1.1	3.9±1.3	670000	470000	530000	41	53	32
	#48	4.0±1.4	3.5±1.0	3.2±1.2	800000	510000	710000	23	38	27
	Mean	3.9	3.1	3.2	805000	510000	632500	34	44	29
	SD <sup>a</sup>	1.5	1.1	1.2	267000	32500	229000	12	7	10
16 Weeks										
Single Lumen	#16	2.6±0.9	2.5±0.8	N/A <sup>b</sup>	370000	380000	1110000	52	31	N/A
12 Weeks										
Single Lumen	#43	N/A	3.5±1.1	N/A	700000	510000	1410000	N/A	51	N/A
8 Weeks										
Single Lumen	#41	N/A	2.6±0.9	3.2±1.1	130000	480000	770000	N/A	29	12
24 Weeks										
Normal Control	#9	— <sup>c</sup>	5.7±1.9	—	—	520000	—	—	44	—

<sup>a</sup>SD=Standard Deviation.

<sup>b</sup>Not Available.

<sup>c</sup>Not Applicable.

Table 4.10: Mean category I axon diameter, nerve area and percentage of nerve observed using SEM

Implant Period & Type of Repair	Animal Number	Mean Axon Diameter ± Standard Deviation ( $\mu\text{m}$ )			Nerve Area ( $\mu\text{m}^2$ )			Percentage of Nerve Examined (%)		
		Prox	Mid	Dist	Prox	Mid	Dist	Prox	Mid	Dist
<b>24 Weeks</b>										
Single Lumen	#5	3.4±1.2	2.4±0.8	2.2±0.9	1180000	550000	380000	1	2	3
	#6	2.9±0.8	2.8±0.9	3.5±0.9	570000	510000	910000	2	2	1
	#47	4.9±1.6	3.6±0.9	3.8±1.0	670000	470000	530000	1	1	2
	#48	3.5±0.9	3.6±1.2	3.6±1.1	800000	510000	710000	1	2	1
	Mean	3.9	3.0	3.1	805000	510000	632500	1	2	2
	SD <sup>a</sup>	1.5	1.1	1.2	267000	32500	229000	1	1	1
<b>16 Weeks</b>										
Single Lumen	#16	2.7±0.8	2.4±0.7	4.0±1.2	370000	380000	1110000	2	3	1
<b>12 Weeks</b>										
Single Lumen	#43	3.0±0.8	3.1±1.0	3.8±1.1	700000	510000	1410000	1	2	1
<b>8 Weeks</b>										
Single Lumen	#41	3.1±1.4	2.9±1.0	2.9±0.8	130000	480000	770000	8	2	1
<b>24 Weeks</b>										
Normal Control	#9	— <sup>b</sup>	5.1±1.8	—	—	520000	—	—	2	—

<sup>a</sup>SD=Standard Deviation.

<sup>b</sup>Not Applicable.

Table 4.11: Mean category II axon diameter, nerve area and percentage of nerve observed using SEM

Implant Period & Type of Repair	Animal Number	Mean Axon Diameter ± Standard Deviation ( $\mu\text{m}$ )			Nerve Area ( $\mu\text{m}^2$ )			Percentage of Nerve Examined (%)		
		Prox	Mid	Dist	Prox	Mid	Dist	Prox	Mid	Dist
24 Weeks										
Single Lumen	#5	3.2±1.3	2.3±0.8	2.7±0.8	1180000	550000	380000	1	2	3
	#6	3.3±1.0	3.4±1.1	3.4±1.1	570000	510000	910000	2	2	1
	#47	5.3±1.6	3.5±1.1	4.7±1.4	670000	470000	530000	1	1	2
	#48	3.6±1.1	3.6±1.1	4.0±1.1	800000	510000	710000	1	2	1
	Mean	4.2	3.1	3.8	805000	510000	632500	1	2	2
	SD <sup>a</sup>	1.6	1.1	1.3	267000	32500	229000	1	1	1
16 Weeks										
Single Lumen	#16	3.0±1.1	2.8±0.8	4.1±1.4	370000	380000	1110000	2	3	1
12 Weeks										
Single Lumen	#43	3.3±1.0	3.4±0.9	4.1±1.2	700000	510000	1410000	1	2	1
8 Weeks										
Single Lumen	#41	3.5±1.0	2.9±1.0	3.2±1.1	130000	480000	770000	8	2	1
24 Weeks										
Normal Control	#9	— <sup>b</sup>	4.9±1.6	—	—	520000	—	—	2	—

<sup>a</sup>SD=Standard Deviation.

<sup>b</sup>Not Applicable.



Table 4.12: Mean total axon diameter, nerve area and percentage of nerve observed using SEM

Implant Period & Type of Repair	Animal Number	Mean Axon Diameter ± Standard Deviation ( $\mu\text{m}$ )			Nerve Area ( $\mu\text{m}^2$ )			Percentage of Nerve Examined (%)		
		Prox	Mid	Dist	Prox	Mid	Dist	Prox	Mid	Dist
		<hr/>								
24 Weeks										
Single Lumen	#5	3.3±1.3	2.3±0.8	2.4±0.9	1180000	550000	380000	1	2	3
	#6	3.2±1.0	3.3±1.1	3.4±1.0	570000	510000	910000	2	2	1
	#47	5.2±1.6	3.5±1.1	4.3±1.3	670000	470000	530000	1	1	2
	#48	3.6±1.0	3.6±1.1	3.8±1.1	800000	510000	710000	1	2	1
	Mean	4.1	3.1	3.4	805000	510000	632500	1	2	2
	SD <sup>a</sup>	1.6	1.1	1.3	267000	32500	229000	1	1	1
<hr/>										
16 Weeks										
Single Lumen	#16	2.9±1.0	2.6±0.8	4.1±1.3	370000	380000	1110000	2	3	1
<hr/>										
12 Weeks										
Single Lumen	#43	3.2±1.0	3.3±1.0	3.9±1.1	700000	510000	1410000	1	2	1
<hr/>										
8 Weeks										
Single Lumen	#41	3.2±1.3	2.9±1.0	3.1±1.0	130000	480000	770000	8	2	1
<hr/>										
24 Weeks										
Normal Control	#9	— <sup>b</sup>	5.0±1.7	—	—	520000	—	—	2	—

<sup>a</sup>SD=Standard Deviation.

<sup>b</sup>Not Applicable.

Table 4.13: Diameter ratio and estimated total axons in each nerve cross section observed using LM

Implant Period & Type of Repair	Animal Number	Diameter Ratio $\pm$ Standard Deviation			Axon Counts (#)		
		Prox	Mid	Dist	Prox	Mid	Dist
24 Weeks							
Single Lumen	#5	1.6 $\pm$ 0.6	2.0 $\pm$ 0.9	1.4 $\pm$ 0.4	17125	12596	8820
	#6	1.8 $\pm$ 0.7	1.6 $\pm$ 0.7	1.8 $\pm$ 0.6	7850	11877	15733
	#47	1.5 $\pm$ 0.5	1.8 $\pm$ 0.8	1.7 $\pm$ 0.5	6829	8287	6638
	#48	1.7 $\pm$ 0.7	1.6 $\pm$ 0.4	1.4 $\pm$ 0.4	9461	8416	12989
	Mean				10316	10294	11045
	SD <sup>a</sup>	— <sup>b</sup>	—	—	4667	2263	4088
16 Weeks							
Single Lumen	#16	1.8 $\pm$ 0.7	1.6 $\pm$ 0.5	N/A <sup>c</sup>	7546	10290	N/A
12 Weeks							
Single Lumen	#43	N/A	1.9 $\pm$ 0.8	N/A	N/A	7980	N/A
8 Weeks							
Single Lumen	#41	N/A	1.5 $\pm$ 0.5	1.7 $\pm$ 0.7	N/A	13310	15517
24 Weeks							
Normal Control	#9	—	1.7 $\pm$ 0.7	—	—	5193	—

<sup>a</sup>SD=Standard Deviation.

<sup>b</sup>Not Applicable.

<sup>c</sup>Not Available.

Table 4.14: Category I axon diameter ratio and estimated total category I axons in each nerve cross section observed using SEM

Implant Period & Type of Repair	Animal Number	Diameter Ratio $\pm$ Standard Deviation			Axon Counts (#)		
		Prox	Mid	Dist	Prox	Mid	Dist
24 Weeks							
Single Lumen	#5	1.6 $\pm$ 0.5	1.7 $\pm$ 0.6	1.6 $\pm$ 0.6	10500	4700	6633
	#6	1.6 $\pm$ 0.5	1.6 $\pm$ 0.6	1.8 $\pm$ 0.6	2650	2100	6600
	#47	1.4 $\pm$ 0.3	1.7 $\pm$ 0.5	1.6 $\pm$ 0.6	6100	4600	3200
	#48	1.7 $\pm$ 0.6	2.0 $\pm$ 0.7	1.5 $\pm$ 0.5	8800	4400	4200
	Mean				7013	3950	5158
	SD <sup>a</sup>	— <sup>b</sup>	—	—	3426	1240	1733
16 Weeks							
Single Lumen	#16	1.8 $\pm$ 0.9	2.0 $\pm$ 1.1	1.6 $\pm$ 0.5	4400	3533	5700
12 Weeks							
Single Lumen	#43	1.5 $\pm$ 0.4	1.6 $\pm$ 0.6	1.9 $\pm$ 0.8	4900	5400	6100
8 Weeks							
Single Lumen	#41	1.8 $\pm$ 0.9	1.4 $\pm$ 0.3	1.9 $\pm$ 0.7	1425	6250	7900
24 Weeks							
Normal Control	#9	—	1.7 $\pm$ 0.5	—	—	3900	—

<sup>a</sup>SD=Standard Deviation.

<sup>b</sup>Not Applicable.

Table 4.15: Category II axon diameter ratio and estimated total category II axons in each nerve cross section observed using SEM

Implant Period & Type of Repair	Animal Number	Diameter Ratio $\pm$ Standard Deviation			Axon Counts (#)		
		Prox	Mid	Dist	Prox	Mid	Dist
<b>24 Weeks</b>							
Single Lumen	#5	1.5 $\pm$ 0.3	1.6 $\pm$ 0.5	1.4 $\pm$ 0.5	7200	9350	3967
	#6	1.3 $\pm$ 0.2	1.3 $\pm$ 0.2	1.5 $\pm$ 0.4	8200	9800	10700
	#47	1.5 $\pm$ 0.5	1.7 $\pm$ 0.6	1.5 $\pm$ 0.4	12900	13300	3250
	#48	1.5 $\pm$ 0.4	1.8 $\pm$ 0.5	1.6 $\pm$ 0.5	10000	5100	7000
	Mean				9575	9388	6229
	SD <sup>a</sup>	_____ <sup>b</sup>	_____	_____	2501	3360	3395
<b>16 Weeks</b>							
Single Lumen	#16	1.4 $\pm$ 0.4	1.6 $\pm$ 0.5	1.5 $\pm$ 0.5	6550	5967	9800
<b>12 Weeks</b>							
Single Lumen	#43	1.6 $\pm$ 0.5	1.5 $\pm$ 0.3	1.6 $\pm$ 0.8	15300	6600	7000
<b>8 Weeks</b>							
Single Lumen	#41	1.6 $\pm$ 0.5	1.5 $\pm$ 0.5	1.4 $\pm$ 0.4	1063	8650	12400
<b>24 Weeks</b>							
Normal Control	#9	_____	1.7 $\pm$ 0.4	_____	_____	1150	_____

<sup>a</sup>SD=Standard Deviation.

<sup>b</sup>Not Applicable.

Table 4.16: Axon diameter ratio and estimated total axons in each nerve cross section observed using SEM

Implant Period & Type of Repair	Animal Number	Diameter Ratio $\pm$ Standard Deviation			Axon Counts (#)		
		Prox	Mid	Dist	Prox	Mid	Dist
<b>24 Weeks</b>							
Single Lumen	#5	1.6 $\pm$ 0.4	1.6 $\pm$ 0.5	1.5 $\pm$ 0.6	17700	14050	10600
	#6	1.4 $\pm$ 0.3	1.4 $\pm$ 0.4	1.6 $\pm$ 0.5	10850	11900	17300
	#47	1.4 $\pm$ 0.4	1.7 $\pm$ 0.6	1.6 $\pm$ 0.5	19000	17900	6450
	#48	1.6 $\pm$ 0.5	1.9 $\pm$ 0.6	1.6 $\pm$ 0.5	18800	9500	11200
	Mean				16588	13338	11388
	SD <sup>a</sup>	— <sup>b</sup>	—	—	3867	3564	4472
<b>16 Weeks</b>							
Single Lumen	#16	1.6 $\pm$ 0.7	1.8 $\pm$ 0.8	1.5 $\pm$ 0.5	10950	9500	15500
<b>12 Weeks</b>							
Single Lumen	#43	1.6 $\pm$ 0.5	1.5 $\pm$ 0.5	1.7 $\pm$ 0.8	20200	12000	13100
<b>8 Weeks</b>							
Single Lumen	#41	1.7 $\pm$ 0.8	1.5 $\pm$ 0.4	1.6 $\pm$ 0.6	2488	14900	20300
<b>24 Weeks</b>							
Normal Control	#9	—	1.7 $\pm$ 0.5	—	—	5050	—

<sup>a</sup>SD=Standard Deviation.

<sup>b</sup>Not Applicable.

not the mean differences were significant for each type of axon in the three nerve sections in each animal. For each section in repaired nerves, the means of the two types of axons were compared, respectively, with those in the normal control. In addition, the means of the total axons obtained in the three sections in each repaired nerve were compared with each other as well as with the normal control. Finally, the means of the total axons observed using SEM were compared with those obtained using LM in the present study. The statistical comparisons can be seen in Table 4.17 through Table 4.24.

#### **4.3.1 Quantitative results from LM**

Approximately 30 to 50 percent of areas in each nerve section were analyzed. The Tukey's test showed that all sections tested from the single-lumen cuff repaired nerves over the four time periods had significantly lower mean axon core diameters than the normal control (Table 4.17). Among the three sections of the 24 week post-implantation nerve cases, the axon core diameters were the largest at the proximal sites as compared to the middle and distal sections (Table 4.18). However, the mean core diameter of the regenerated axons did not reach the normal control level size even after 24 weeks.

Reciprocal relationships between the axons per unit area calculations and the mean axon core diameters were found in the nerve sections of 24 week post-implantation rats; i.e., the larger the mean axon core diameter became, the smaller the number for the axons per unit area. The numerical value of the axons per unit area in the normal control was smaller than that

Table 4.17: Mean axon diameter comparisons between repaired nerve sections and normal control observed using LM

Animal Number	Type of Repair	Implant Periods	Section Comparisons <sup>a</sup>	Significance <sup>b</sup>
#41	Single-lumen	8 Weeks	P	N/A
			M	*** (p<0.0001) (+)
			D	*** (p<0.0001) (+)
#43	Single-lumen	12 Weeks	P	N/A
			M	*** (p<0.0001) (+)
			D	N/A
#16	Single-lumen	16 Weeks	P	*** (p<0.05) (+)
			M	*** (p<0.05) (+)
			D	N/A
#5	Single-lumen	24 Weeks	P	*** (p<0.0001) (+)
			M	*** (p<0.0001) (+)
			D	*** (p<0.0001) (+)
#6	Single-lumen	24 Weeks	P	*** (p<0.0001) (+)
			M	*** (p<0.0001) (+)
			D	*** (p<0.0001) (+)
#47	Single-lumen	24 Weeks	P	*** (p<0.0001) (+)
			M	*** (p<0.0001) (+)
			D	*** (p<0.0001) (+)
#48	Single-lumen	24 Weeks	P	*** (p<0.0001) (+)
			M	*** (p<0.0001) (+)
			D	*** (p<0.0001) (+)

<sup>a</sup>P=Proximal; M=Middle; D=Distal; Comparing the sections with normal control.

<sup>b</sup>N/A=Not Available; (+) Larger mean axon diameters in normal control.

\*\*\* Comparisons significant at the 0.05 level, p value in brackets.

Table 4.18: Mean axon diameter comparisons between nerve sections in the same animal observed using LM

Animal Number	Type of Repair	Implant Periods	Section Comparisons <sup>a</sup>	Significance <sup>b</sup>
#41	Single-lumen	8 Weeks	P, M	N/A
			P, D	N/A
			M, D	*** (p<0.0001) (-)
#43	Single-lumen	12 Weeks	P, M	N/A
			P, D	N/A
			M, D	N/A
#16	Single-lumen	16 Weeks	P, M	*** (p<0.01) (+)
			P, D	N/A
			M, D	N/A
#5	Single-lumen	24 Weeks	P, M	*** (p<0.0001) (+)
			P, D	*** (p<0.0001) (+)
			M, D	*
#6	Single-lumen	24 Weeks	P, M	*** (p<0.0001) (+)
			P, D	*** (p<0.0001) (+)
			M, D	*** (p<0.0001) (-)
#47	Single-lumen	24 Weeks	P, M	*** (p<0.001) (+)
			P, D	*** (p<0.001) (+)
			M, D	*** (p<0.001) (-)
#48	Single-lumen	24 Weeks	P, M	*** (p<0.0001) (+)
			P, D	*** (p<0.0001) (+)
			M, D	*** (p<0.0001) (+)

<sup>a</sup>P=Proximal; M=Middle; D=Distal.

<sup>b</sup>N/A=Not Available; (+) Larger mean axon diameters in the first nerve section; (-) Larger mean axon diameters in the second nerve section.

\*\*\* Comparisons significant at the 0.05 level, p value in brackets.

\* Comparisons not significant at the 0.05 level.



Table 4.19: Mean diameter comparisons of the same category of axons in repaired nerve sections and in normal control observed using SEM

Animal Number	Type of Repair	Implant Periods	Nerve Section <sup>a</sup>	Axon Comparisons <sup>b</sup>	Significance <sup>c</sup>
#41	Single-lumen	8 Weeks	P	I	*** (p<0.05) (+)
			P	II	*** (p<0.05) (+)
			M	I	*** (p<0.05) (+)
			M	II	*** (p<0.05) (+)
			D	I	*** (p<0.05) (+)
			D	II	*** (p<0.05) (+)
#43	Single-lumen	12 Weeks	P	I	*** (p<0.05) (+)
			P	II	*** (p<0.05) (+)
			M	I	*** (p<0.05) (+)
			M	II	*** (p<0.05) (+)
			D	I	*** (p<0.05) (+)
			D	II	*
#16	Single-lumen	16 Weeks	P	I	*** (p<0.05) (+)
			P	II	*** (p<0.05) (+)
			M	I	*** (p<0.05) (+)
			M	II	*** (p<0.05) (+)
			D	I	*** (p<0.05) (+)
			D	II	*** (p<0.05) (+)

<sup>a</sup>P=Proximal; M=Middle; D=Distal.

<sup>b</sup>I=Category I axons; II=Category II axons; Comparing axons in the nerve sections with those in normal control.

<sup>c</sup>(+) Larger mean axon diameters in normal control.

\*\*\* Comparisons significant at the 0.05 level, p value in brackets.

\* Comparisons not significant at the 0.05 level.

Table 4.19: Continued

Animal Number	Type of Repair	Implant Periods	Nerve Section <sup>a</sup>	Axon Comparisons <sup>b</sup>	Significance <sup>c</sup>
#5	Single-lumen	24 Weeks	P	I	*** (p<0.01) (+)
			P	II	*** (p<0.01) (+)
			M	I	*** (p<0.01) (+)
			M	II	*** (p<0.01) (+)
			D	I	*** (p<0.01) (+)
			D	II	*** (p<0.01) (+)
#6	Single-lumen	24 Weeks	P	I	*** (p<0.01) (+)
			P	II	*** (p<0.01) (+)
			M	I	*** (p<0.01) (+)
			M	II	*** (p<0.01) (+)
			D	I	*** (p<0.01) (+)
			D	II	*** (p<0.01) (+)
#47	Single-lumen	24 Weeks	P	I	*
			P	II	*
			M	I	*** (p<0.0001) (+)
			M	II	*** (p<0.0001) (+)
			D	I	*** (p<0.0001) (+)
			D	II	*
#48	Single-lumen	24 Weeks	P	I	*** (p<0.05) (+)
			P	II	*** (p<0.05) (+)
			M	I	*** (p<0.05) (+)
			M	II	*** (p<0.05) (+)
			D	I	*** (p<0.05) (+)
			D	II	*** (p<0.05) (+)

Table 4.20: Mean axon diameter comparisons between repaired nerve sections and normal control observed using SEM

Animal Number	Type of Repair	Implant Periods	Section Comparisons <sup>a</sup>	Significance <sup>b</sup>
#41	Single-lumen	8 Weeks	P	*** (p<0.0001) (+)
			M	*** (p<0.0001) (+)
			D	*** (p<0.0001) (+)
#43	Single-lumen	12 Weeks	P	*** (p<0.0001) (+)
			M	*** (p<0.0001) (+)
			D	*** (p<0.0001) (+)
#16	Single-lumen	16 Weeks	P	*** (p<0.0001) (+)
			M	*** (p<0.0001) (+)
			D	*** (p<0.0001) (+)
#5	Single-lumen	24 Weeks	P	*** (p<0.0001) (+)
			M	*** (p<0.0001) (+)
			D	*** (p<0.0001) (+)
#6	Single-lumen	24 Weeks	P	*** (p<0.0001) (+)
			M	*** (p<0.0001) (+)
			D	*** (p<0.0001) (+)
#47	Single-lumen	24 Weeks	P	*
			M	*** (p<0.0001) (+)
			D	*** (p<0.0001) (+)
#48	Single-lumen	24 Weeks	P	*** (p<0.0001) (+)
			M	*** (p<0.0001) (+)
			D	*** (p<0.0001) (+)

<sup>a</sup>P=Proximal; M=Middle; D=Distal; Comparing the sections with normal control.

<sup>b</sup>(+) Larger mean axon diameters in normal control.

\*\*\* Comparisons significant at the 0.05 level, p value in brackets.

\* Comparisons not significant at the 0.05 level.

Table 4.21: Diameter comparisons between the category I and the category II axons in the same nerve section observed using SEM

Animal Number	Type of Repair	Implant Periods	Nerve Section <sup>a</sup>	Significance <sup>b</sup>
#41	Single-lumen	8 Weeks	P	*
			M	*
			D	*
#43	Single-lumen	12 Weeks	P	*
			M	*
			D	*
#16	Single-lumen	16 Weeks	P	*
			M	*
			D	*
#5	Single-lumen	24 Weeks	P	*
			M	*
			D	*** (p<0.05) (+)
#6	Single-lumen	24 Weeks	P	*
			M	*
			D	*
#47	Single-lumen	24 Weeks	P	*
			M	*
			D	*** (p<0.0001) (+)
#48	Single-lumen	24 Weeks	P	*
			M	*
			D	*
#9	Normal Control	24 Weeks	M	*

<sup>a</sup>P=Proximal; M=Middle; D=Distal.

<sup>b</sup>(+) Larger mean axon diameters in category II axons.

\*\*\* Comparisons significant at the 0.05 level, p value in brackets.

\* Comparisons not significant at the 0.05 level.

Table 4.22: Mean diameter comparisons of the same category of axons in different nerve sections observed using SEM

Animal Number	Type of Repair	Implant Periods	Section Comparisons <sup>a</sup>	Axon Type <sup>b</sup>	Significance <sup>c</sup>
#41	Single-lumen	8 Weeks	P, M	I	*
			P, M	II	*** (p<0.05) (+)
			P, D	I	*
			P, D	II	*
			M, D	I	*
			M, D	II	*
#43	Single-lumen	12 Weeks	P, M	I	*
			P, M	II	*
			P, D	I	*** (p<0.05) (-)
			P, D	II	*** (p<0.05) (-)
			M, D	I	*** (p<0.05) (-)
			M, D	II	*** (p<0.05) (-)
#16	Single-lumen	16 Weeks	P, M	I	*
			P, M	II	*
			P, D	I	*** (p<0.05) (-)
			P, D	II	*** (p<0.05) (-)
			M, D	I	*** (p<0.05) (-)
			M, D	II	*** (p<0.05) (-)

<sup>a</sup> P=Proximal; M=Middle; D=Distal.

<sup>b</sup> I=Category I axons; II=Category II axons.

<sup>c</sup> (+) Larger mean axon diameters in the first nerve section; (-) Larger mean axon diameters in the second nerve section.

\*\*\* Comparisons significant at the 0.05 level, p value in brackets.

\* Comparisons not significant at the 0.05 level.

Table 4.22: Continued

Animal Number	Type of Repair	Implant Periods	Section Comparisons <sup>a</sup>	Axon Type <sup>b</sup>	Significance <sup>c</sup>
#5	Single-lumen	24 Weeks	P, M	I	*** (p<0.01) (+)
			P, M	II	*** (p<0.01) (+)
			P, D	I	*** (p<0.01) (+)
			P, D	II	*** (p<0.01) (+)
			M, D	I	*
			M, D	II	*
#6	Single-lumen	24 Weeks	P, M	I	*
			P, M	II	*
			P, D	I	*** (p<0.01) (-)
			P, D	II	*
			M, D	I	*** (p<0.01) (-)
			M, D	II	*
#47	Single-lumen	24 Weeks	P, M	I	*** (p<0.0001) (+)
			P, M	II	*** (p<0.0001) (+)
			P, D	I	*** (p<0.0001) (+)
			P, D	II	*** (p<0.0001) (+)
			M, D	I	*
			M, D	II	*** (p<0.0001) (-)
#48	Single-lumen	24 Weeks	P, M	I	*
			P, M	II	*
			P, D	I	*
			P, D	II	*
			M, D	I	*
			M, D	II	*

Table 4.23: Mean diameter of total axons comparisons between nerve sections in the same animal observed using SEM

Animal Number	Type of Repair	Implant Periods	Section Comparisons <sup>a</sup>	Significance <sup>b</sup>
#41	Single-lumen	8 Weeks	P, M	*** (p<0.0001) (+)
			P, D	*
			M, D	*
#43	Single-lumen	12 Weeks	P, M	*
			P, D	*** (p<0.0001) (-)
			M, D	*** (p<0.0001) (-)
#16	Single-lumen	16 Weeks	P, M	*
			P, D	*** (p<0.0001) (-)
			M, D	*** (p<0.0001) (-)
#5	Single-lumen	24 Weeks	P, M	*** (p<0.0001) (+)
			P, D	*** (p<0.0001) (+)
			M, D	*
#6	Single-lumen	24 Weeks	P, M	*
			P, D	*
			M, D	*
#47	Single-lumen	24 Weeks	P, M	*** (p<0.0001) (+)
			P, D	*** (p<0.0001) (+)
			M, D	*** (p<0.0001) (-)
#48	Single-lumen	24 Weeks	P, M	*
			P, D	*
			M, D	*

<sup>a</sup>P=Proximal; M=Middle; D=Distal.

<sup>b</sup>(+) Larger mean axon diameters in the first nerve section; (-) Larger mean axon diameters in the second nerve sections.

\*\*\* Comparisons significant at the 0.05 level, p value in brackets.

\* Comparisons not significant at the 0.05 level.

Table 4.24: Diameter comparisons of axons in the same nerve section observed from LM and SEM

Animal Number	Type of Repair	Implant Periods	Section Comparisons <sup>a</sup>	Significance <sup>b</sup>
#41	Single-lumen	8 Weeks	P	N/A
			M	*** (p<0.0001) (-)
			D	*
#43	Single-lumen	12 Weeks	P	N/A
			M	*** (p<0.0001) (+)
			D	N/A
#16	Single-lumen	16 Weeks	P	*** (p<0.0001) (-)
			M	*
			D	N/A
#5	Single-lumen	24 Weeks	P	*
			M	*** (p<0.0001) (+)
			D	*** (p<0.0001) (+)
#6	Single-lumen	24 Weeks	P	*** (p<0.0001) (+)
			M	*** (p<0.0001) (-)
			D	*
#47	Single-lumen	24 Weeks	P	*** (p<0.0001) (-)
			M	*
			D	*** (p<0.0001) (-)
#48	Single-lumen	24 Weeks	P	*** (p<0.0001) (+)
			M	*
			D	*** (p<0.0001) (-)
#9	Normal Control	24 Weeks	M	*** (p<0.0001) (+)

<sup>a</sup>P=Proximal; M=Middle; D=Distal.

<sup>b</sup>N/A=Not Available; (+) Larger mean axon diameter in LM; (-) Larger mean axon diameters in SEM.

\*\*\* Comparisons significant at the 0.05 level, p value in brackets.

\* Comparisons not significant at the 0.05 level.



in any regenerated nerve section. Moreover, the number for the axons per unit area at the middle section in each repaired animal was larger than that at the proximal section. Large variations were seen for comparisons of the estimated total number of axons in different nerve sections.

The average diameter ratios in all of the nerve sections including the normal control were between 1.4 and 2.0. Thus, the shapes of the axons in the rats were substantially different from that of a circle where the value would be 1.0.

#### **4.3.2 Quantitative results from SEM**

Less than ten percent of the areas in each nerve section were analyzed. When comparing the category I and II axons in most of the repaired nerve sections, a significantly larger mean diameter was seen in the normal control (Table 4.19). Similar results were seen as when the mean diameter of the total axons in each nerve section was compared with that of the normal control (Table 4.20). In the same nerve sections for each animal, no significant mean diameter differences were noted between the category I and the category II axons except in the distal sites of animal #5 and animal #47 (Table 4.21). Both exceptions were caused by the skewing of the distributions of category II axons to larger axon diameters as compared with those of the category I axons. Large variations were seen for comparisons of the same category of axons in different nerve sections (Table 4.22), and for comparisons of the mean diameters of total axons between nerve sections in the same animal (Table 4.23). Finally, some significant differences were

seen for comparisons of the mean axon diameters obtained by using LM and SEM (Table 4.24).

The numerical values of axons per unit area of the category II and the total axons at the three sections in each repaired animal were larger than that of the normal control. There were still large variations in the numerical values of axons per unit area and in the estimated total number of axons among the three sections in each animal.

The average diameter ratios for the category I, the category II, and the total axons in all nerve sections including the normal control were between 1.3 and 2.0. Again, these shapes show a substantial departure from that of a circle where the ratio would be 1.0.

## 5. DISCUSSION

The peripheral nerve regeneration of this study centered on the use of single lumen silicone rubber tubes. The tube functioned as a conduit for the regenerating nerve, providing longitudinal support and control of the orientation for migrating cells and growing axons. The growth environment was isolated from the extraneural environment. The results showed that a 5 mm gap between the proximal and the distal stumps was successfully bridged by a structure composed of regenerating axons.

Secondary electron images were not as useful in characterizing the axon features as were the backscatter electron images. The backscatter electron images provided useful contrast between the relatively low average atomic number of the connective tissue and that of the silver stained (gold toned) axons.

Backscatter electron images provided structural information for axon features not easily seen in light microscopy. The present study showed the existence of stained features that did not cover a full circular axon cross-section, but would be counted and interpreted as a full cross-section in convention light microscopic characterization of stained axon cross sections. The proportion of these features to that of complete axon cross sections was provided. The results suggested that they represented a stage in the development of the argyrophilic protein of the axons.

Two patterns of regenerated features were recognized: the axons fully surrounded by the endoneurium (category I) and those in which staining enhanced rim features or only a portion of the circular area (category II),

which could not be discriminated by light microscopy but were observed using SEM in studying the proximal, middle, and distal sections of the repaired nerves. The category I axons are probably the axons growing faster during the regenerative process which have completely matured. The category II axon cross sections are probably related to the type of neurofilament proteins that developed during the regenerative process. Neurofilament proteins in the axons have a high affinity for free silver ions. Therefore, immature axons might contain fewer argyrophilic neurofilament proteins to pick up the silver ions that would make up a cross section and so the area would be only partially stained by the Bodian's silver method (Katz and Watson, 1985). Another possibility for the formation of category II axon cross sections is that the regenerating axons did not grow straight but in a spiral manner within the basal lamina tubes (Tohyama and Kumagai, 1992). Thus, there can be seen unstained spaces between the growing axons and the basal lamina tubes in certain cross sections. A portion of the category II axons in which staining enhanced only rim features may be the open endoneurial tubes left after severance of a nerve and subsequent degeneration, providing channels for the regenerating axons to grow into the distal nerve stump. In addition, these axon features may be caused by the sectioning, pulling out some of the axon material from the endoneurial tubes, and perhaps forming the rim-stained features. Moreover, a component of these axons are likely to be unmyelinated axons and collapsed capillaries.

Instead of forming one central, large nerve fascicle at the three nerve sections as seen in the normal control, the regenerated axons grouped in

small packets which were separated by a wide area of connective tissue. Similar findings have been reported for "mini-fascicles" formation during nerve regeneration across a gap (Mathur et al., 1983; Jenq and Coggeshall, 1986).

The fiber diameter histograms obtained from the light and scanning electron micrographs provided evidence that the regenerated nerve was comprised primarily of smaller fibers than those at the time the nerve gap was created because the histogram of the regenerated nerve was shifted to the left in comparison with that of the normal control. More than 60% of axon diameter distributions were within  $\pm 1 \mu\text{m}$  of the mean axon diameters in each nerve section except the normal control which had a pattern suggesting the presence of a bimodal distribution and the proximal section in animal #47 which had a wide spread distribution. The results showed that the majority of regenerating axons achieved an axon diameter frequency distribution which had a substantial peak occurring at the mean diameter value of the regenerating axons. Small regenerated axons which were less than  $1 \mu\text{m}$  in diameter were not included in the histograms. Small regenerated axons with few neurofilament proteins would not be stained by the silver-stain method (Katz and Watson, 1985), and few were seen in the SEM images. Thus, any small axons (less than  $1 \mu\text{m}$  in diameter) were also omitted in the graphs for data of the LM studies.

In the repaired nerve, myelinated fibers are undergoing degeneration and remyelination at the same time. Quantitative results obtained by using LM and SEM showed that complete recovery of these fibers, as defined by an increase in axonal diameter compared to normal dimensions was never

achieved at 24 weeks post-implantation, the longest time period of the present study. The diminished average regenerated axon size agrees with the observations of Mira (1979), Henry et al. (1985), Espejo and Alvarez (1986), and Le Beau et al. (1988) for similar age control rat comparisons in that the regenerated myelinated fibers never reach the normal average size, even after long implantation times of the order of two years. In addition, the mean diameters of the middle section axons were smaller than those of the proximal sections in almost all of the single cuff experimental animals. The trend of smaller mean axon diameters occurring in the middle sections could be because the repair cuffs might cause an environment of compression of the regenerating axons and therefore limit the sizes of these axons. Also, the development of capillaries and blood vessels in the middle sections might not be as extensive as for the proximal or distal sections. The middle section in each animal had an equal or a larger numerical value for axons per unit area compared with that of the proximal section. This may represent more proximal axons with successful growth into the repair site, or this may represent more branching of middle axons. No significant differences were seen for comparisons of the mean diameters of axons in category I with those of the axons in category II. This may suggest that these two categories of axons are probably the same type of axons even though their shapes or morphological features are different. Significant differences were noted between the quantitative data obtained from light and scanning electron micrographs in the present study, such as the axon populations, mean axon diameters, and the numerical values of axons per unit area. This could be because the total size of the area using the SEM represented only a small

fraction of the nerve sample (<10%) in comparison with that for the LM. There was a possibility that the SEM areas scanned did not include enough axons for an adequate evaluation compared to the larger LM areas.

The mean diameter ratios at the three nerve sections in each animal including the normal control were larger than one. These results were not in accord with some studies in which the regenerated fibers were more circular, lacking the irregular fluted appearance of the normal fibers (Mackinnon et al., 1985, O'Brien et al., 1987).

## 6. CONCLUSIONS

Both LM and SEM micrographs showed that the single-lumen cuff experiments were successful in bridging the 5 mm gap in the sciatic nerve of the rat at all four post-implantation periods as based on the presence of silver stained axons seen in cross sections of proximal, middle (covering the gap region), and distal samples.

Two regenerative features, the axons fully surrounded by the endoneurium and those in which staining enhanced rim features or only a portion of the circular area, were seen in the high-resolution backscatter electron micrographs. These were not distinguishable using light microscopy. The differences in morphology of the two categories of axons may be caused by several things: staining and sectioning or growth of the regenerating axons within the basal lamina tubes. The two categories of axons comprise the axons seen in LM.

Based on the LM and SEM results, higher numerical values of axons per unit area for the cross-sections of the regenerated nerves were seen compared to those for the normal control. In addition, mean regenerated axon diameters did not reach sizes similar to those of the control for each of the four time periods. The higher numerical values of axons per unit area and smaller mean axon diameters in the regenerated nerves compared to the control indicate some branching during the regenerative process.

There are many more proximal axons than those that enter or pass through the lumen of the single lumen cuffs, and the surface area of the proximal stump is larger than the cross-sectional area of the nerve in the



middle section. However, higher numerical values for axons per unit area measurements in the middle sections of the regenerated nerves as compared with those in the proximal sections may represent proximal axons with successful growth into the repair site that result in a higher value of axons per unit area in the middle section. No excessive branching was evident in the distal sections since no significant changes of axon densities occurred in the distal sections as compared with those in the middle sections.

Significant differences were seen for the data comparisons from LM and SEM. This could be because the SEM areas seen represented only a portion of those included in the LM study.

**BIBLIOGRAPHY**

- Allt, G. 1976. Pathology of the peripheral nerve. Page 722 in D. N. Landon, ed. *The Peripheral Nerve*. John Wiley and Sons, Inc., New York.
- Braley, S. 1970. The chemistry and properties of the medical-grade silicones. *J. Macromol. Sci.-Chem.* A4(3): 529-544.
- Byrkit, D. R., 1987. *Statistics Today*. The Benjamin Cummings Publishing Company, Menlo Park, 687-690.
- Calabretta, A. M., B. L. Munger, and W. P. Graham. 1973. The ultrastructure of degenerating rat sciatic nerves. *J. of Surgical Research* 14: 465-471.
- Daniel, J. M. K. 1991. Reorganization and orientation of peripheral nerve fibers regenerating through a multiple-lumen silicone rubber cuff: An experimental study using the sciatic nerve of rats. Ph. D. Dissertation. Iowa State University. 152 pages.
- DeNee, P. B., J. L. Abraham, and P. A. Willard. 1974. Histochemical stains for the scanning electron microscope: Qualitative and semi-quantitative aspects of specific silver stains. *Scanning Electron Microscopy (Part I)*: 259-266.
- Espejo, F., and J. Alvarez. 1986. Microtubules and calibers in normal and regenerating axons of the sural nerve of the rat. *The J. of Comp. Neuro.* 250: 65-72.
- Gershenbaum, M. R., and F. J. Roisen. 1978. A scanning electron microscopic study of peripheral nerve degeneration and regeneration. *Neuroscience* 3: 1241-1250.

- Gibson, K. L., and J. K. Daniloff. 1989. Comparison of sciatic nerve regeneration through silicone tubes and nerve allografts. *Microsurgery* 10: 126-129.
- Henry, E. W., T. H. Chiu, E. Nyilas, T. M. Brushart, P. Dikkes, and R. L. Sidman. 1985. Nerve regeneration through biodegradable polyester tubes. *Exp. Neuro.* 90: 652-676.
- Ide, C., K. Tohyama, R. Yokota, T. Nitatori, and S. Onodera. 1983. Schwann cell basal lamina and nerve regeneration. *Brain Research* 288: 61-75.
- Jenq, C. B., and R. E. Coggeshall. 1984. Regeneration of axons in tributary nerves. *Brain Research* 310: 107-121.
- Jenq, C. B., and R. E. Coggeshall. 1985. Numbers of regenerating axons in parent and tributary peripheral nerves in the rat. *Brain Research* 326: 27-40.
- Jenq, C. B., and R. E. Coggeshall. 1986. The effects of autologous transplant on patterns of regeneration in rat sciatic nerve. *Brain Research* 364: 45-56.
- Jenq, C. B., and R. E. Coggeshall. 1987. Sciatic nerve regeneration after autologous sural nerve transplantation in the rat. *Brain Research* 406: 52-61.
- Katz, M. J., and L. F. Watson. 1985. Intensifier for Bodian staining of tissue sections and cell cultures. *Stain Technology* 60: 81-87.
- Kumagai, K. I., T. Ushiki, K. Tohyama, M. Arakawa, and C. Ide. 1990. Regenerating axons and their growth cones observed by scanning electron microscopy. *J. Electron Microscopy* 39: 108-114.

- Le Beau, J. M., M. H. Ellisman, and H. C. Powell. 1988. Ultrastructural and morphometric analysis of long-term peripheral nerve regeneration through silicone tubes. *J. of Neurocytology* 17: 161-172.
- Lewis, E. R. 1971. Studying neuronal architecture and organization with SEM. *Scanning Electron Microscopy (Part I)*: 281-288.
- Mackinnon, S. E., A. L. Dellon, A. R. Hudson, and D. A. Hunter. 1985. A primate model for chronic nerve compression. *J. of Reconstructive Microsurgery* 1: 185-194.
- Marshall, D. M., M. Grosser, M. C. Stephanides, R. D. Keeley, and J. M. Rosen. 1989. Sutureless nerve repair at the fascicular level using a nerve coupler. *J. of Rehabilitation Research and Development* 26: 63-76.
- Mathur, A., J. C. Merrell, R. C. Russell, and E. G. Zook. 1983. A scanning electron microscopy evaluation of peripheral nerve regeneration. *Scanning Electron Microscopy (Part II)*: 975-981.
- Mira, J. C. 1979. Quantitative studies of the regeneration of rat myelinated nerve fibres: variations in the number and size of regenerating fibres after repeated localized freezings. *J. Anat.* 129: 77-93.
- Miyakawa, T., A. Shimoji, R. Kuramoto, Y. Higuchi, and T. Kubota. 1981. Morphological observations of peripheral nerves by the scanning electron microscope. *Folia Psychiat. Neurol. Japonica.* 35: 501-506.
- O'Brien, J. P., S. E. Mackinnon, and A. R. Maclean. 1987. A model of chronic nerve compression in the rat. *Annals of Plastic Surgery* 19: 430-435.
- O'Daly, J. A., and T. Imaeda. 1967. Electron microscopic study of Wallerian degeneration in cutaneous nerves caused by mechanical injury. *Laboratory Investigation* 17: 744-766.

- Orgel, M. G., and J. W. Huser. 1980. A comparison of light and scanning electron microscopy in nerve regeneration studies. *Plastic and Reconstructive Surgery* 65: 628-634.
- Phillips, L. L., L. Autilio-Gambetti, and R. J. Lasek. 1983. Bodian's silver method reveals molecular variation in the evolution of neurofilament proteins. *Brain Research* 278: 219-223.
- Rosen, J. M., V. R. Hentz, and E. N. Kaplan. 1983. Fascicular tubulization: A cellular approach to peripheral nerve repair. *Annals of Plastic Surgery* 11: 397-411.
- Rosen, J. M., H. N. Pham, G. Abraham, L. Harold, and V. R. Hentz. 1989. Artificial nerve graft compared to autograft in a rat model. *J. of Rehabilitation Research* 26: 1-14.
- Rosen, J. M., J. A. Padilla, K. D. Nguyen, J. Siedman, and H. N. Pham. 1992. Artificial nerve graft using glycolide trimethylene carbonate as a nerve conduit filled with collagen compared to sutured autograft in a rat model. *J. of Rehabilitation Research* 29: 1-12.
- Satou, T., S. Nishida, S. Hiruma, K. Tanji, M. Takahashi, S. Fujita, Y. Mizuhara, F. Akai, and S. Hashimoto. 1986. A morphological study on the effects of collagen gel matrix on regeneration of severed rat sciatic nerve in silicone tubes. *Acta Pathol. Jpn.* 36: 199-208.
- Seckel, B. R., T. H. Chiu, E. Nyilas, and R. L. Sidman. 1984. Nerve regeneration through synthetic biodegradable nerve guides: Regulation by the target organ. *Plastic and Reconstructive Surgery* 74: 173-181.
- Spencer, P. S. 1977. Morphology of the injured peripheral nerve. Page 345 in R. K. Daniel and J. K. Terzis, eds. *Reconstructive Microsurgery*. Little, Brown and Company, Boston.

- Swaim, S. F. 1987. Peripheral nerve surgery. Pages 493-512 in J. E. Oliver, B. F. Hoerlein, and I. G. Mayhew, eds. *Veterinary Neurology*. W. B. Saunders Company, Philadelphia.
- Taylor, J. S. H., J. W. Fawcett, and L. Hirst. 1984. The use of backscattered electrons to examine selectively stained nerve fibers in the scanning electron microscope. *Stain Technology* 59: 335-341.
- Tohyama, K., A. R. Lieberman, and C. Ide. 1986. Immunohistochemical studies of peripheral nerve regeneration. In: T. Imura, S. Maruse, T. Suzuki, eds. *Proceedings of the XIth International Congress on Electron Microscopy*. *Journal of Electron Microscopy* 35 (supplement), 3209-3210.
- Tohyama, K., and K. I. Kumagai. 1992. Backscattered electron imaging by scanning electron microscopy of regenerating peripheral nerve axons immunostained with antineurofilament antibody. *J. Electron Microscopy* 41: 397-401.
- Valentini, R. E., P. Aebischer, S. R. Winn, and P. M. Galletti. 1987. Collagen- and laminin-containing gels impede peripheral nerve regeneration through semipermeable nerve guidance channels. *Exp. Neuro.* 98: 350-356.
- Van Noort, R., and M. M. Black. 1981. Silicone rubbers for medical applications. Pages 79-98 in D. F. William, eds. *Biocompatibility of Clinical Implant Materials*. CRC Press Inc., Florida.
- Von Langsdorff, D., S. S. Ali, and F. Nürnbergger. 1990. An improved silver staining technique as an alternative nuclear or combined nuclear nerve-fiber impregnation for comparative light-, secondary and backscattered electron scanning microscopy. *J. of Neuroscience Methods* 35: 3-8.

Waller, A. 1850. Experiments on the section of glossopharyngeal and hypoglossal nerves of the frog, and observations of the alterations produced thereby in the structure of their primitive fibers. *Philos. Trans. R. Soc. Lond. [Biol.]* 140: 423-429.

Wolman, M. 1955. Studies of the impregnation of nervous tissue elements, I. Impregnation of axons and myelin. *Quarterly J. of Microscopical Science* 96: 329-336.

## **ACKNOWLEDGEMENTS**

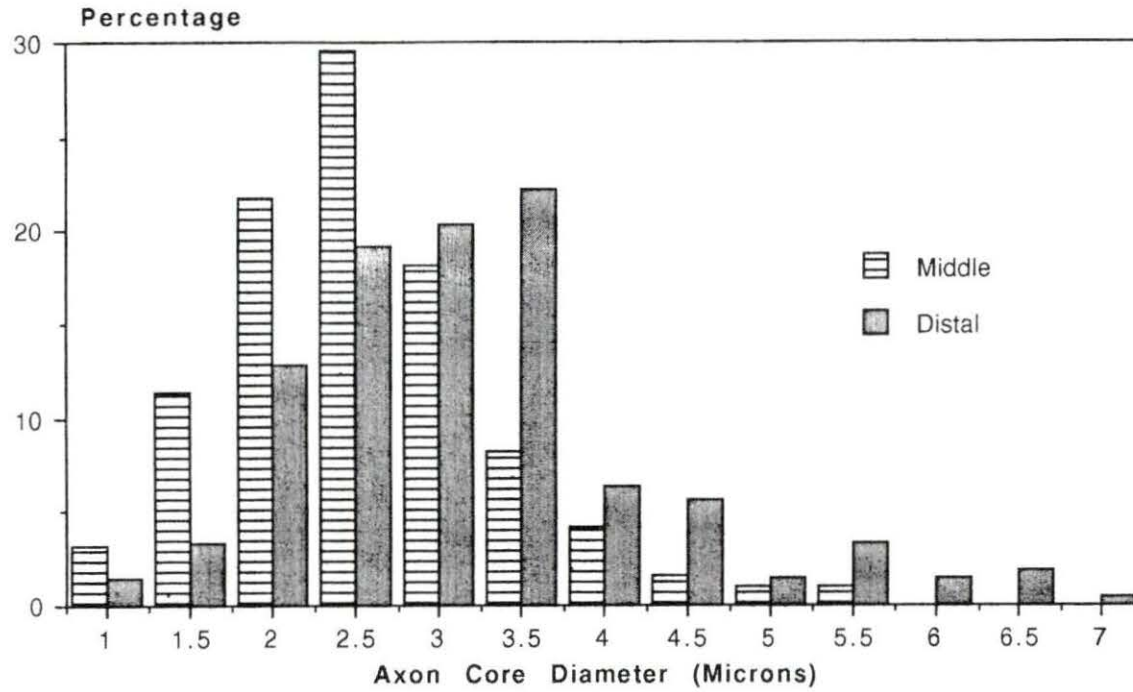
I express my sincere thanks to my major professor, Dr. Raymond T. Greer, for suggesting the project and for his patient encouragement and guidance throughout the course of my graduate study. I would also like to thank Dr. Mary Helen Greer and Frederick Hembrough for serving as members of my committee.

Finally, I would most like to thank my parents, my sister, and my wife for the constant encouragement and support they have given me throughout my studies.

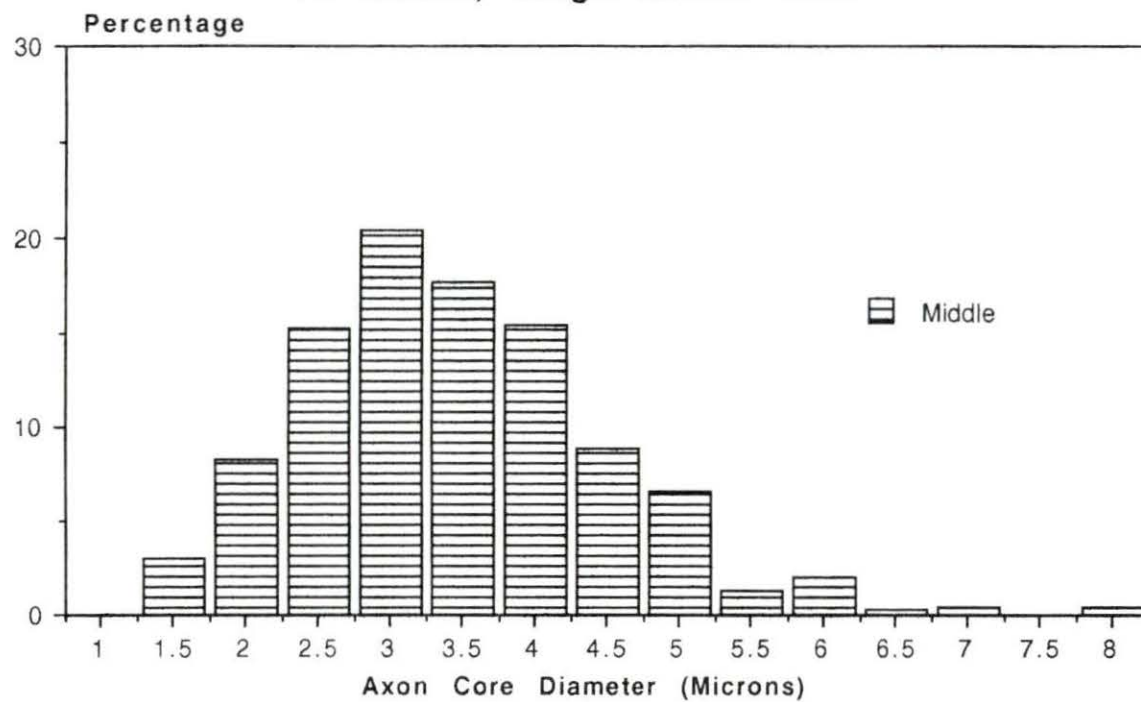


**APPENDIX: FIBER DIAMETER HISTOGRAMS**

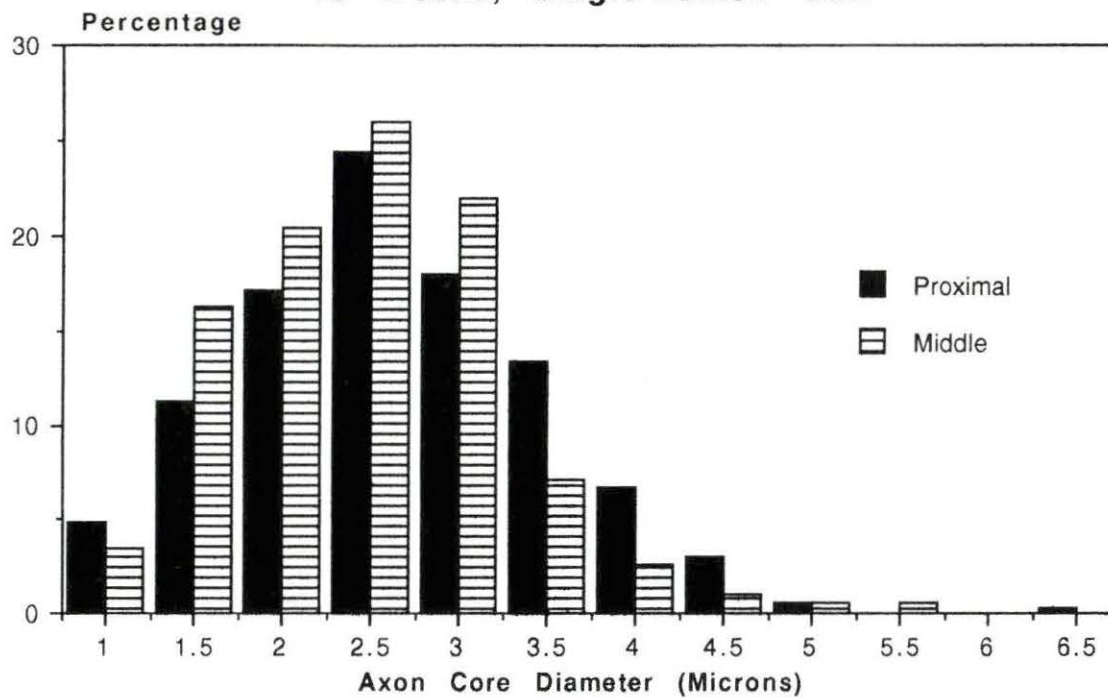
**Axon Diameter Distribution  
Animal #41, LM  
8 Weeks, Single-Lumen Cuff**



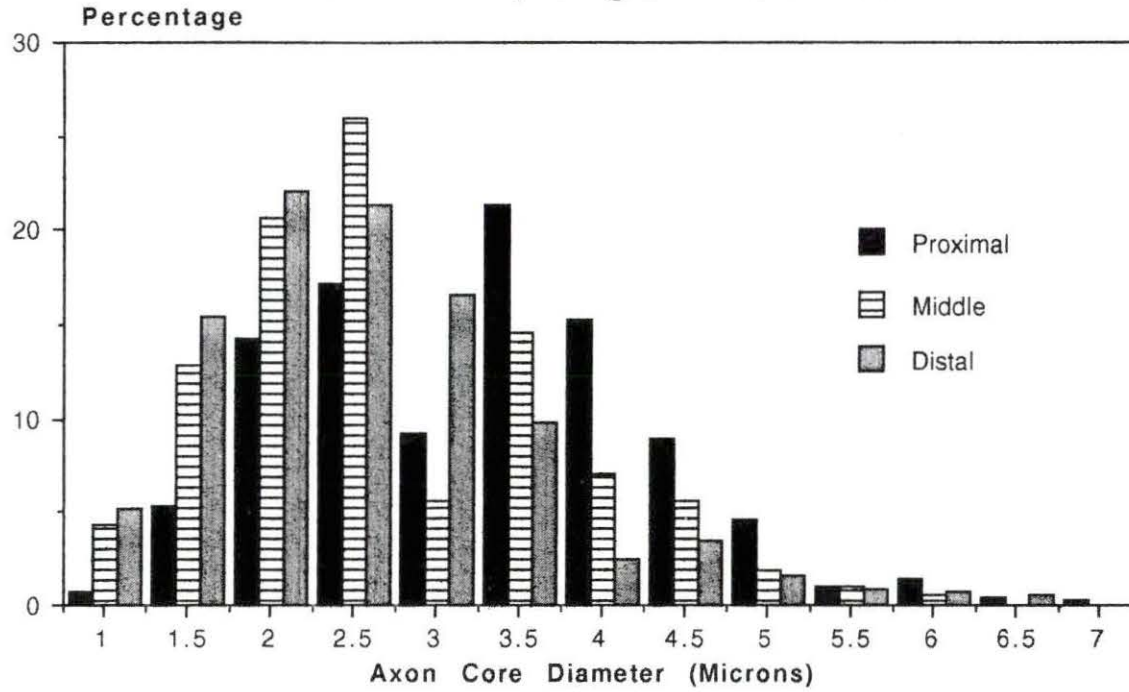
**Axon Diameter Distribution**  
**Animal #43, LM**  
**12 Weeks, Single-Lumen Cuff**



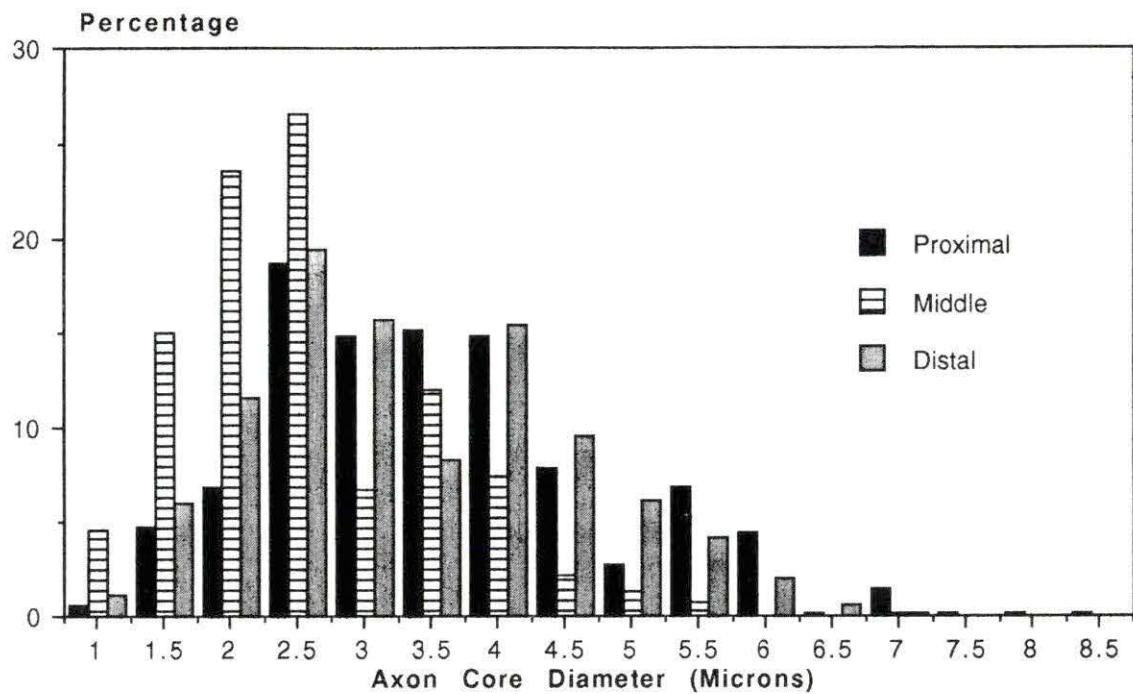
**Axon Diameter Distribution  
Animal #16, LM  
16 Weeks, Single-Lumen Cuff**



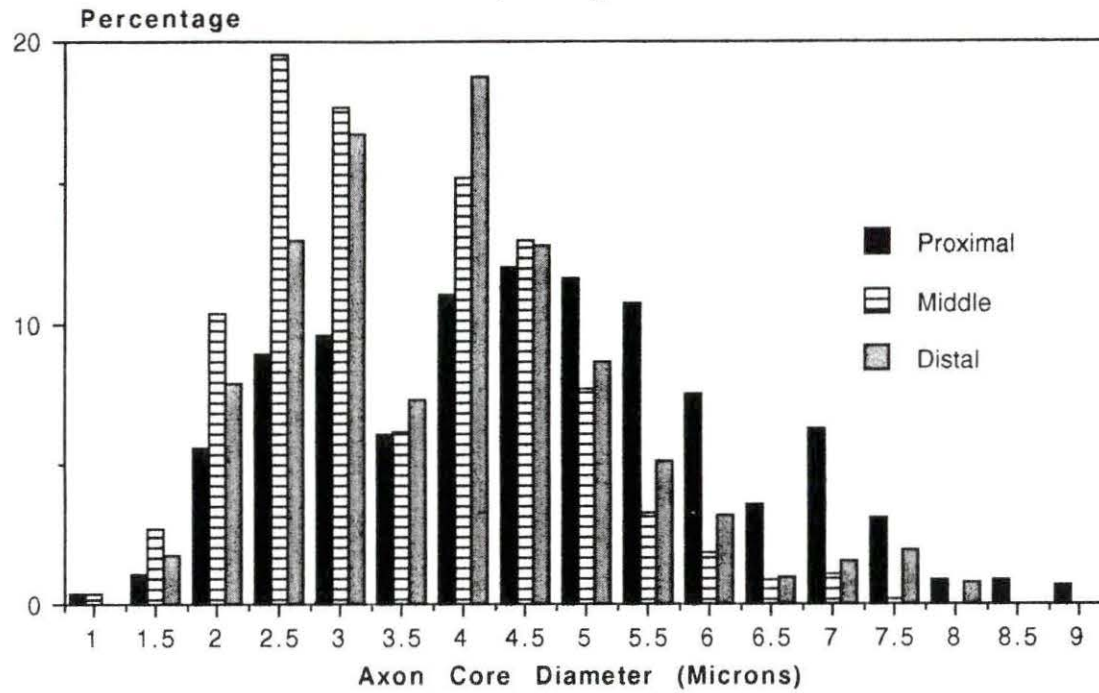
**Axon Diameter Distribution  
Animal #5, LM  
24 Weeks, Single-Lumen Cuff**



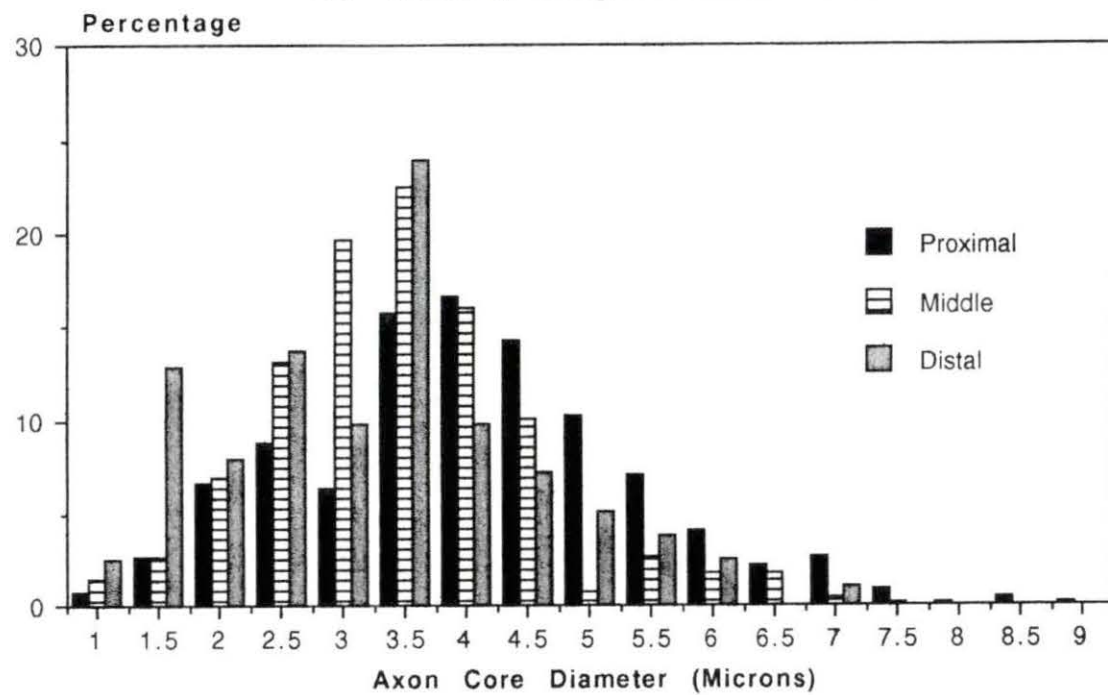
**Axon Diameter Distribution  
Animal #6, LM  
24 Weeks, Single-Lumen Cuff**



**Axon Diameter Distribution  
Animal #47, LM  
24 Weeks, Single-Lumen Cuff**

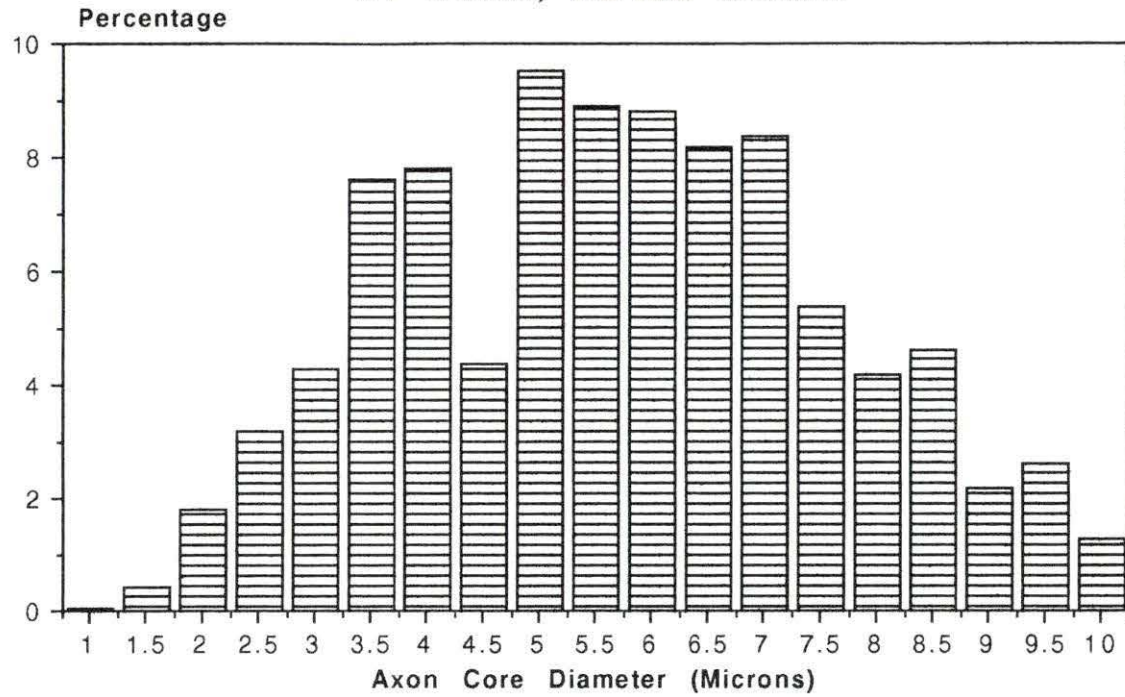


**Axon Diameter Distribution  
Animal #48, LM  
24 Weeks, Single-Lumen Cuff**

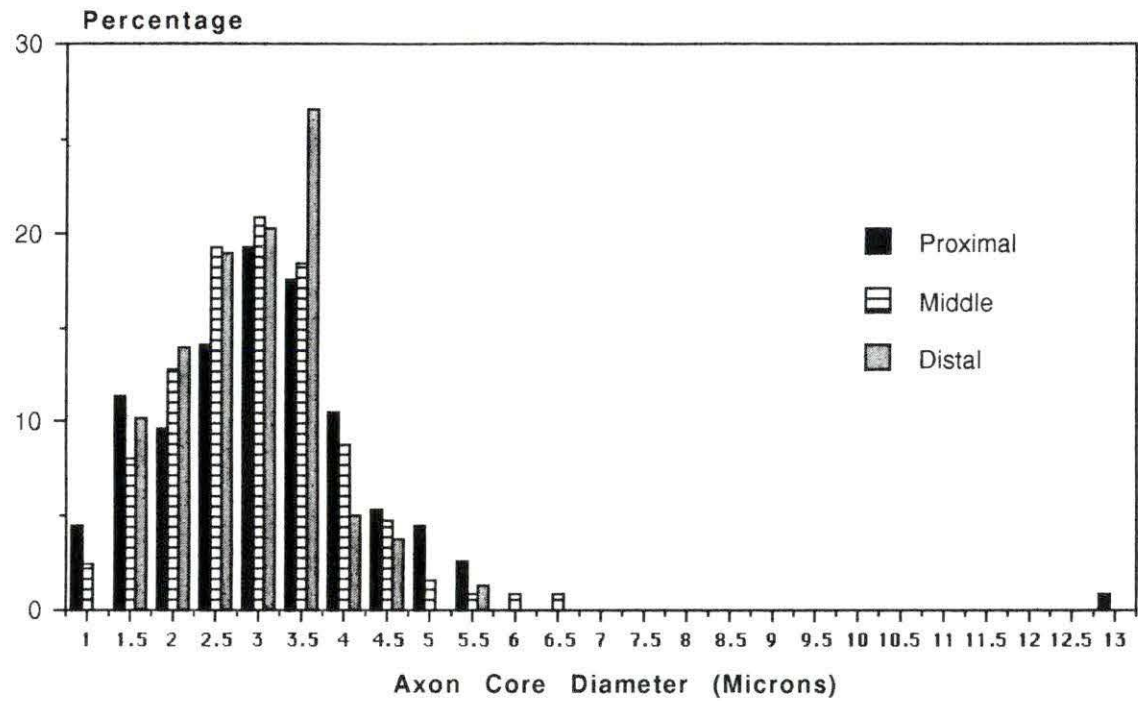




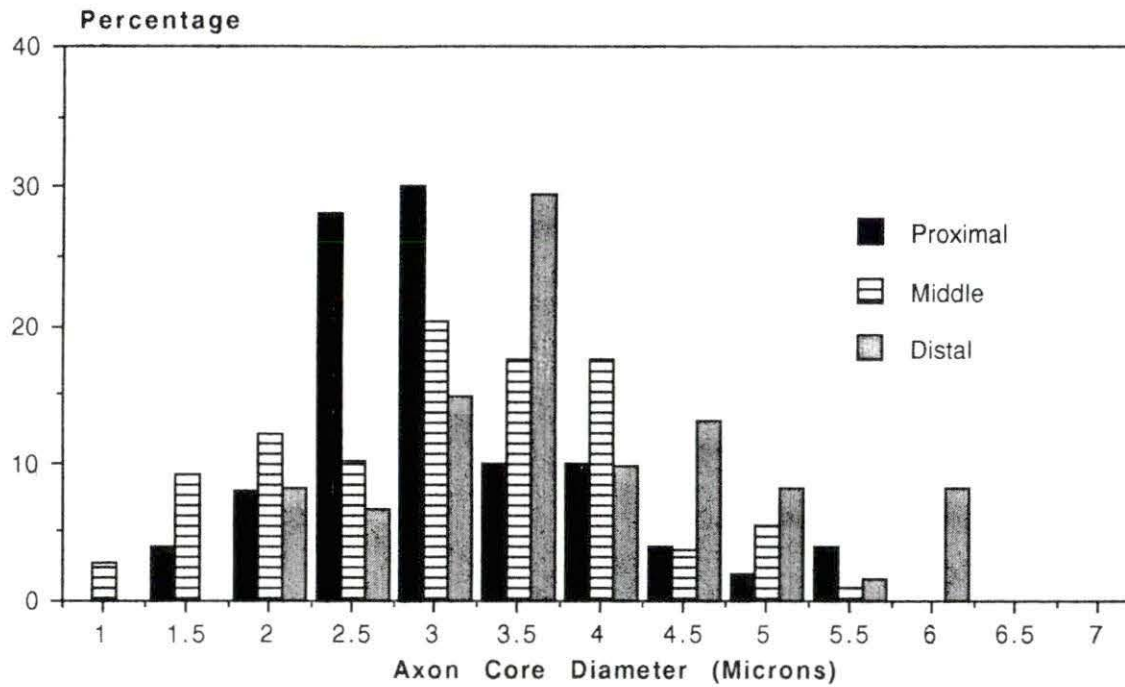
**Axon Diameter Distribution**  
**Animal #9, LM**  
**24 Weeks, Normal Control**



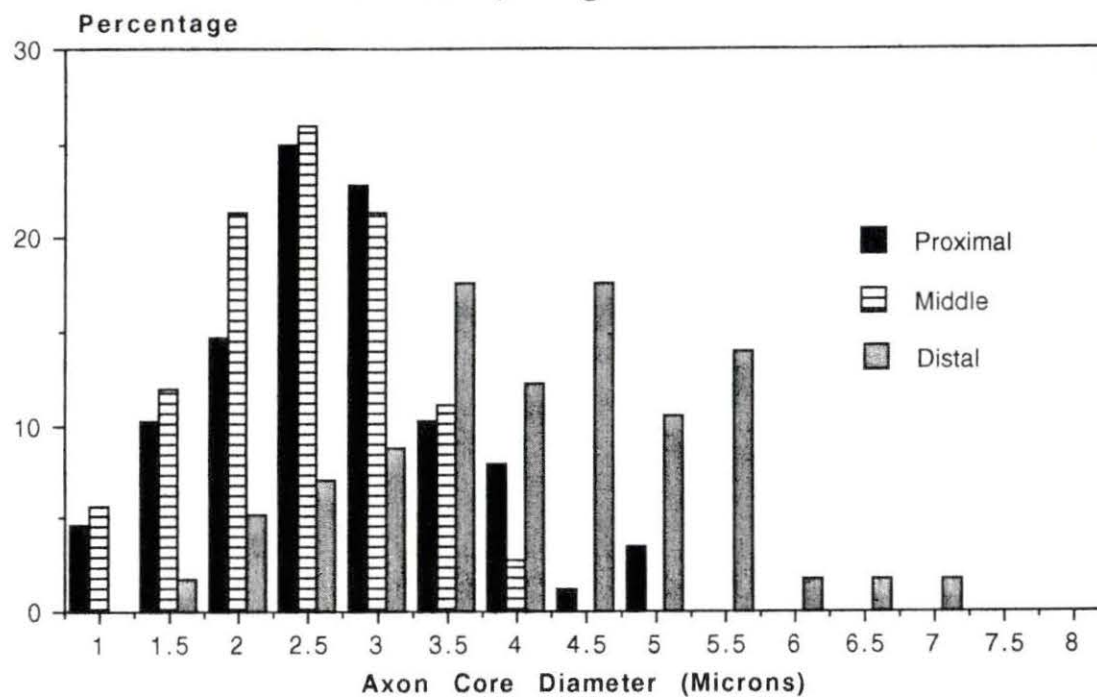
Category I Axon Diameter Distribution  
Animal #41, SEM  
8 Weeks, Single-Lumen Cuff



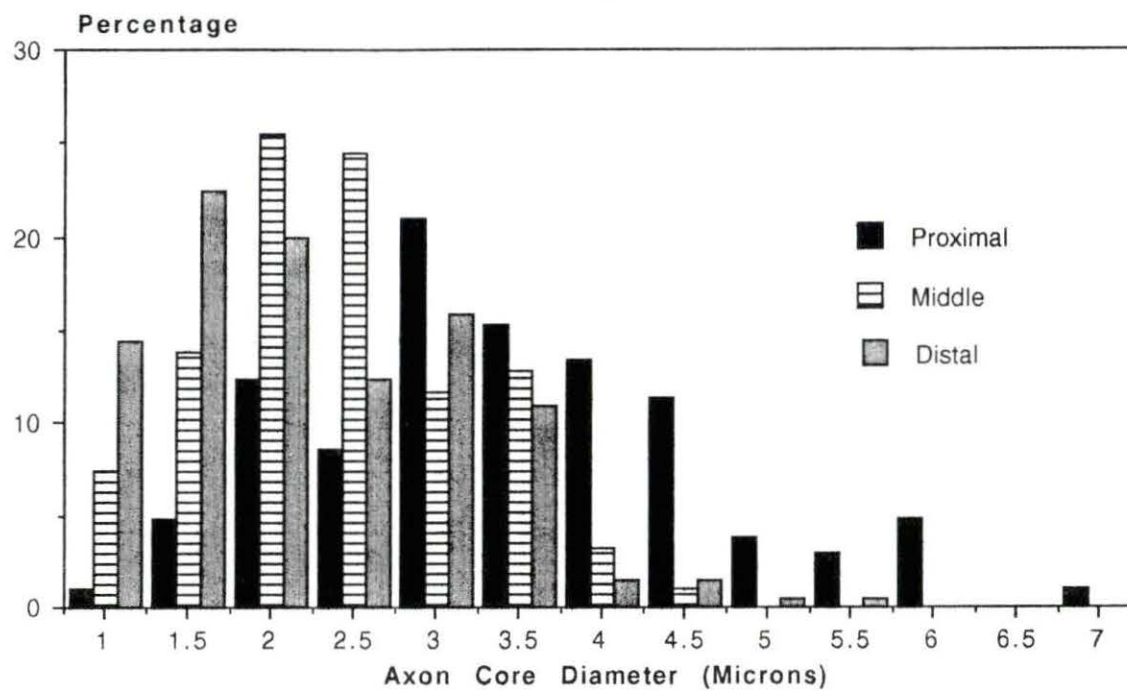
Category I Axon Diameter Distribution  
Animal #43, SEM  
12 Weeks, Single-Lumen Cuff



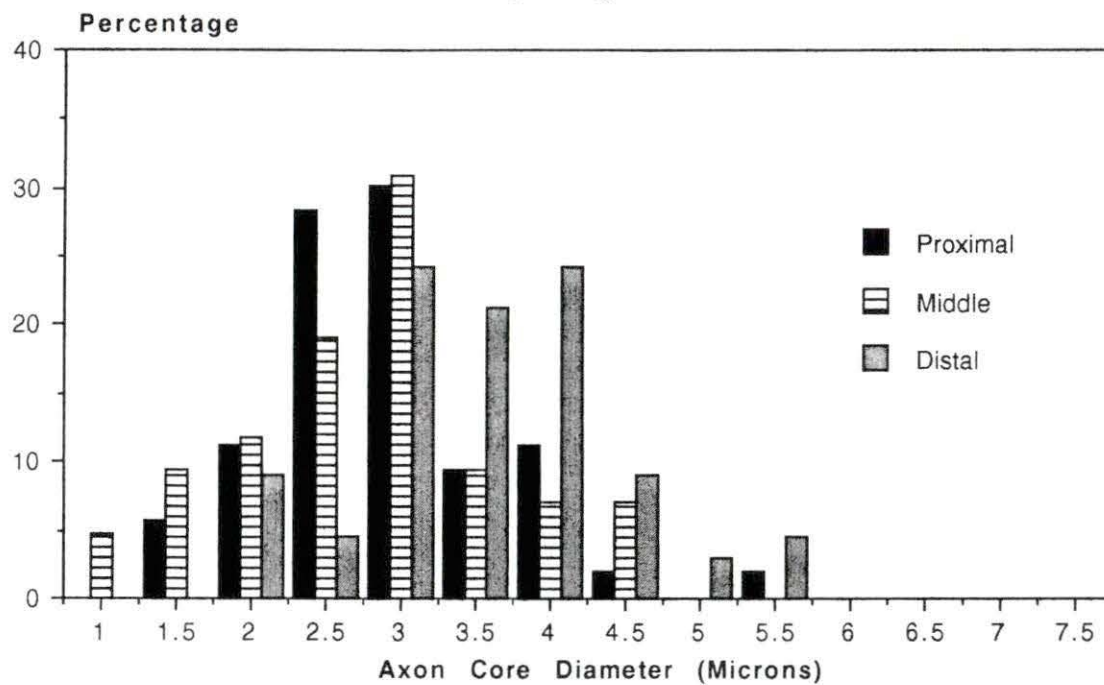
Category I Axon Diameter Distribution  
Animal #16, SEM  
16 Weeks, Single-Lumen Cuff



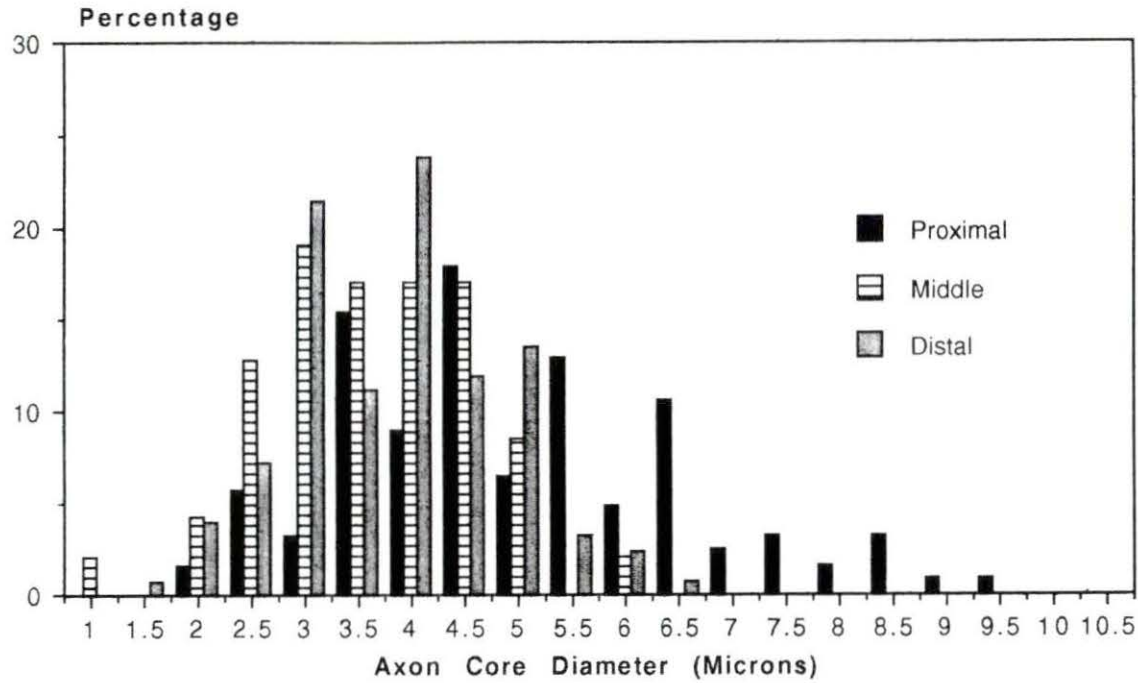
Category I Axon Diameter Distribution  
Animal #5, SEM  
24 Weeks, Single-Lumen Cuff



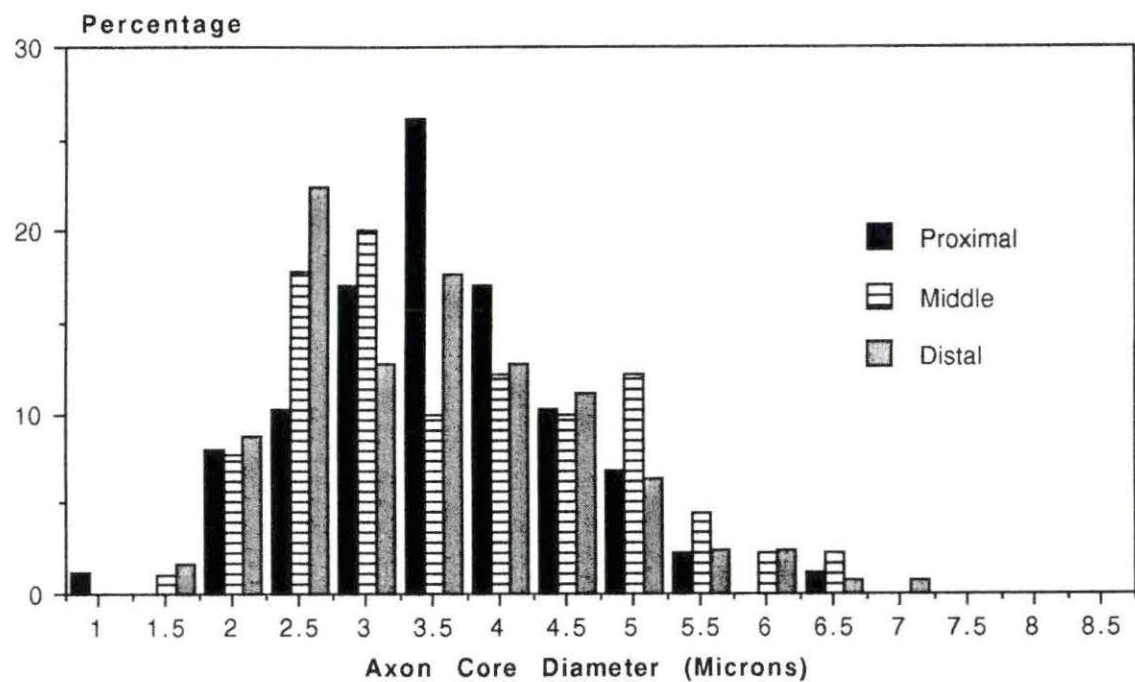
Category I Axon Diameter Distribution  
Animal #6, SEM  
24 Weeks, Single-Lumen Cuff



Category I Axon Diameter Distribution  
Animal #47, SEM  
24 Weeks, Single-Lumen Cuff

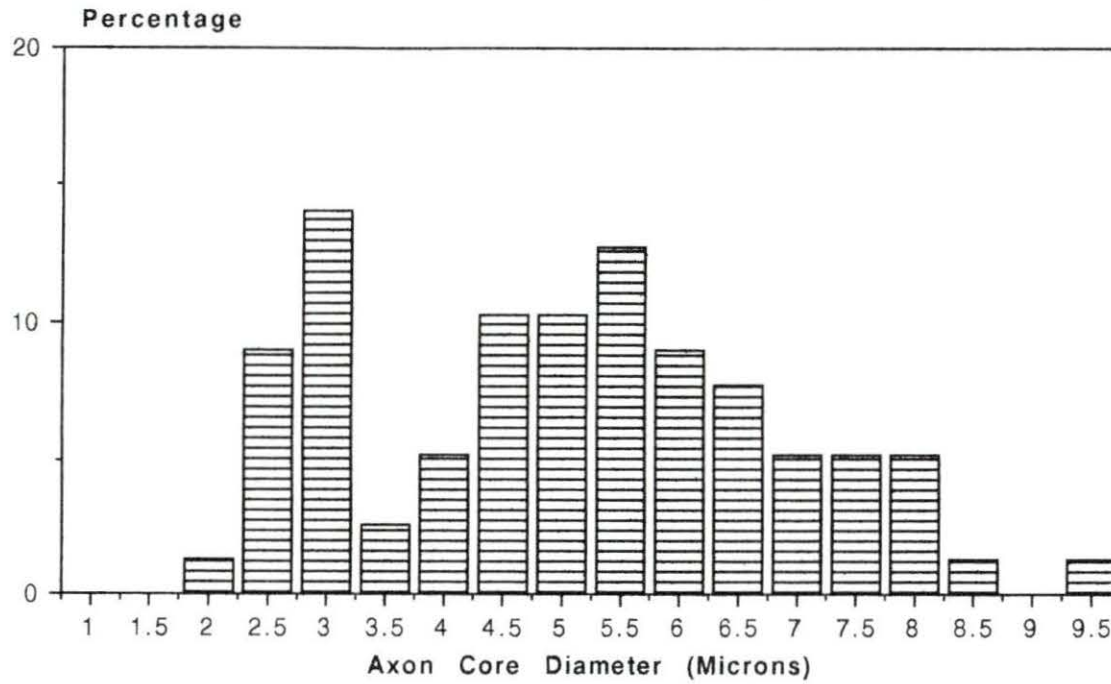


Category I Axon Diameter Distribution  
Animal #48, SEM  
24 Weeks, Single-Lumen Cuff

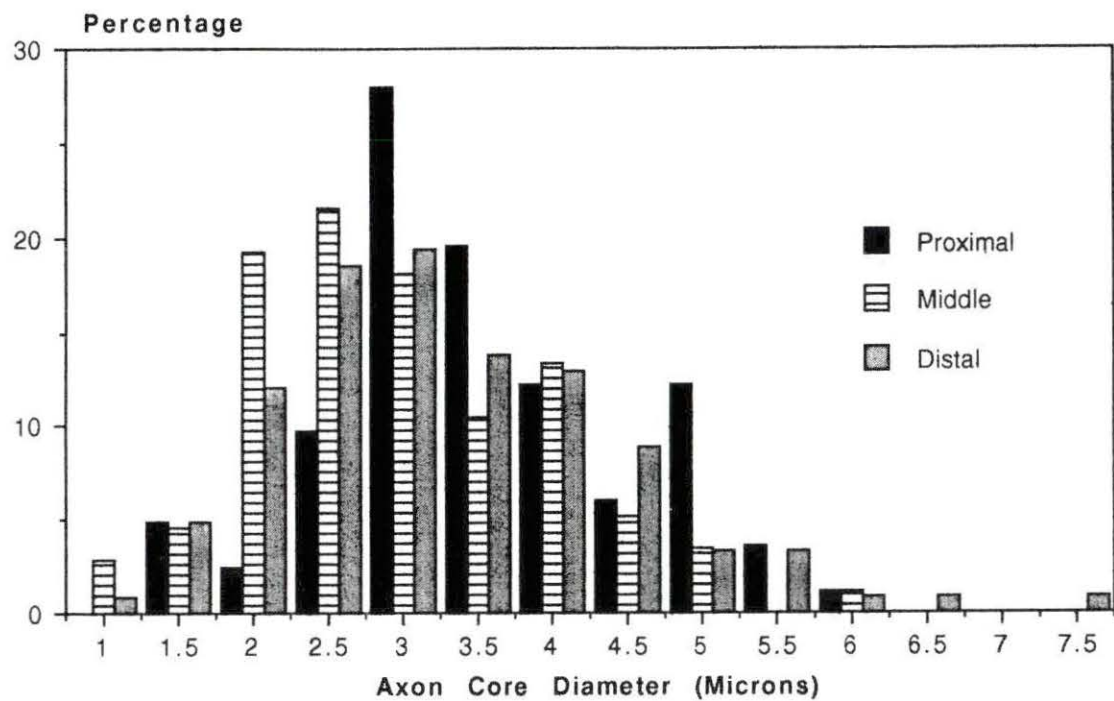




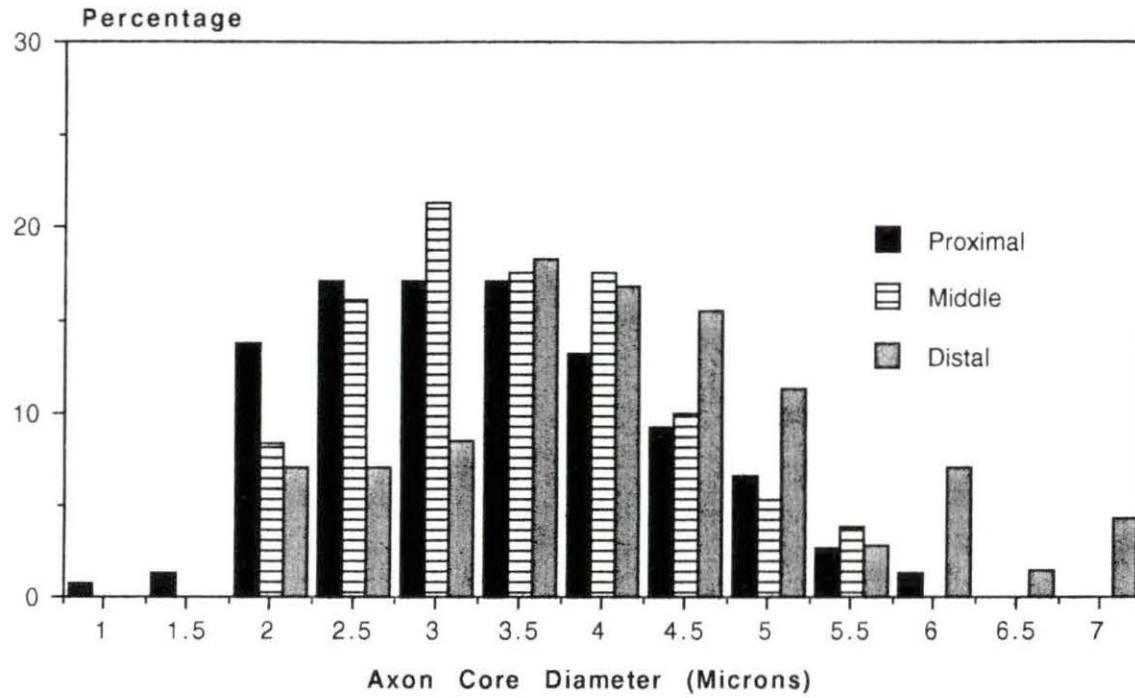
**Category I Axon Diameter Distribution  
Animal #9, SEM  
24 Weeks, Normal Control**



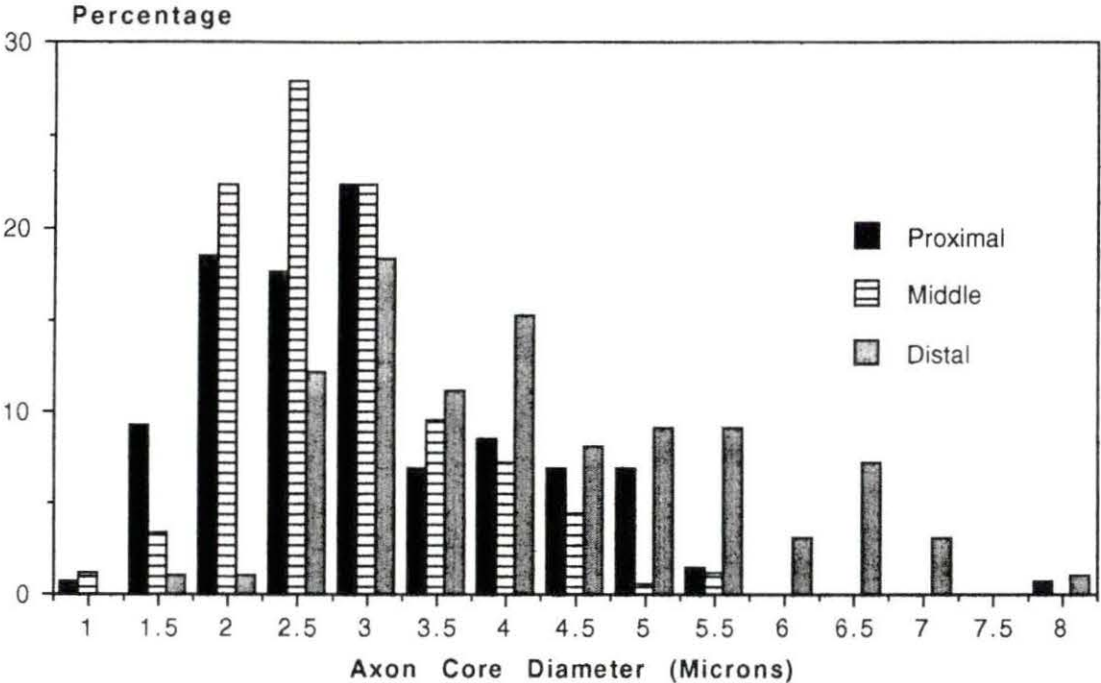
**Category II Axon Diameter Distribution**  
**Animal #41, SEM**  
**8 Weeks, Single-Lumen Cuff**



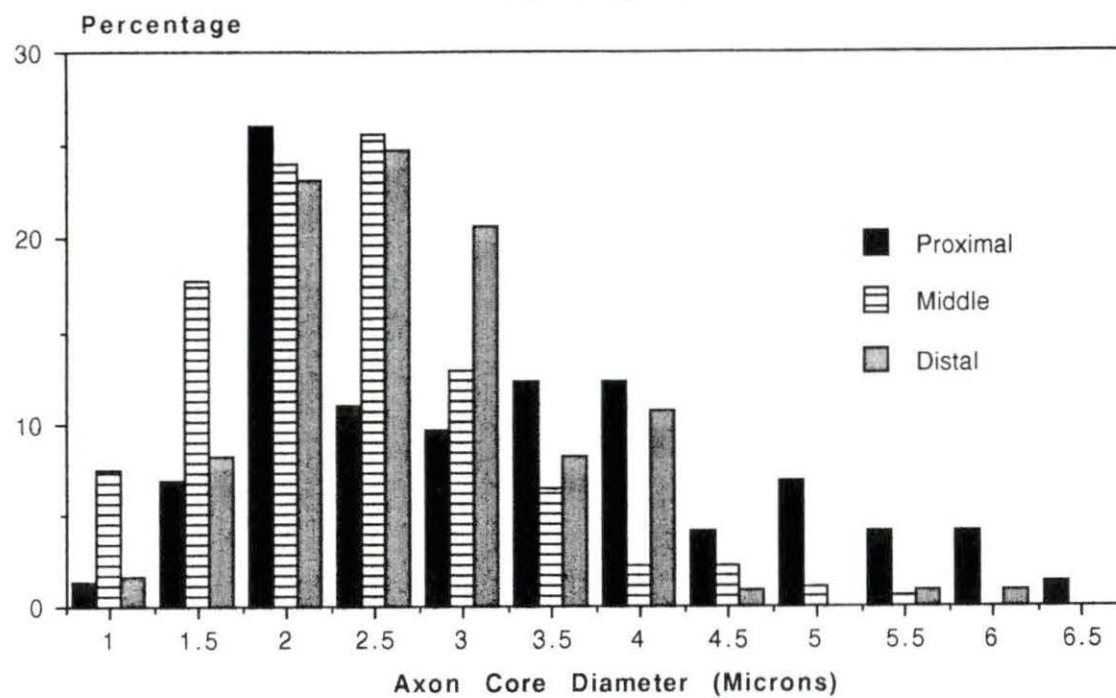
Category II Axon Diameter Distribution  
Animal #43, SEM  
12 Weeks, Single-Lumen cuff



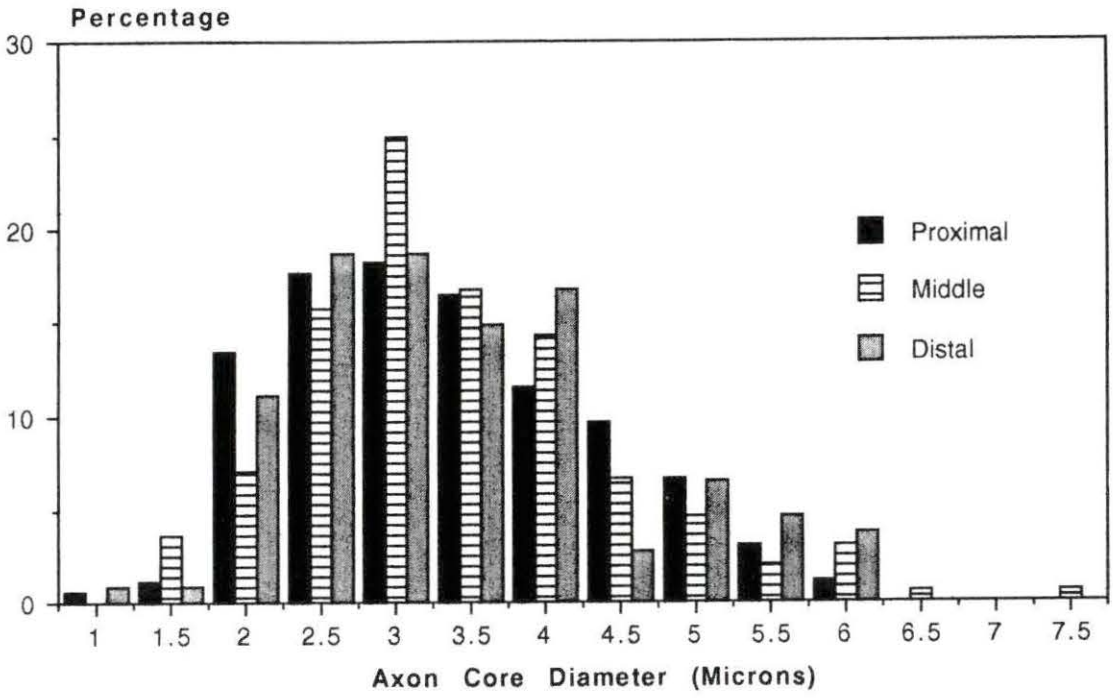
**Category II Axon Diameter Distribution  
Animal #16, SEM  
16 Weeks, Single-Lumen Cuff**



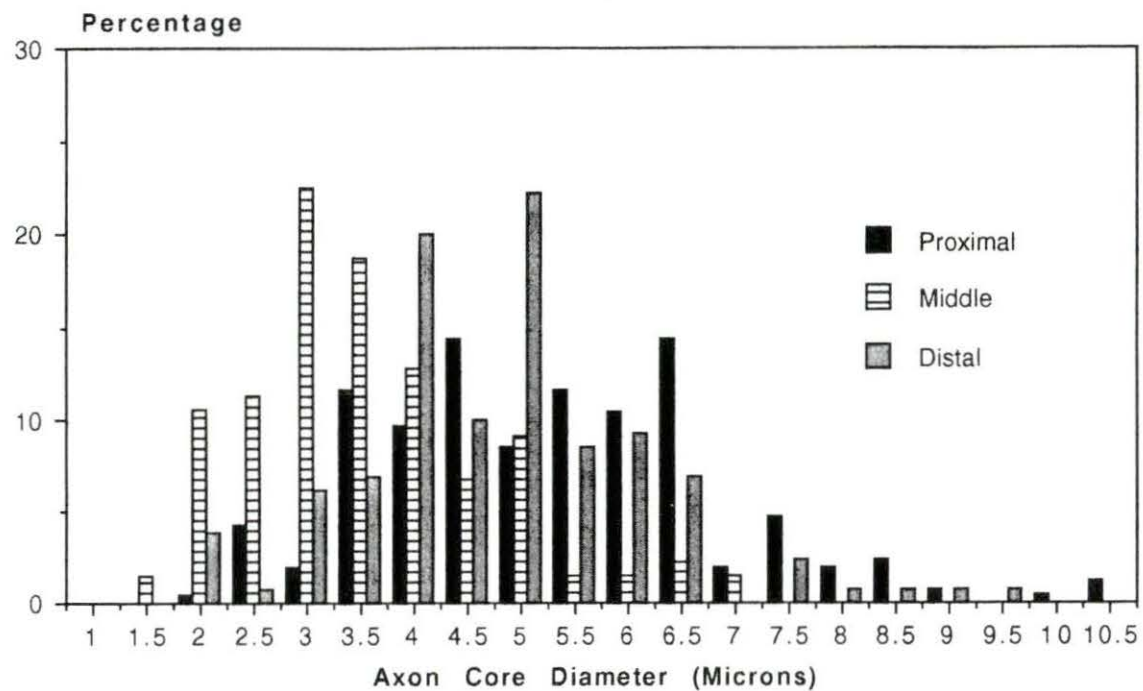
Category II Axon Diameter Distribution  
Animal #5, SEM  
24 Weeks, Single-Lumen Cuff



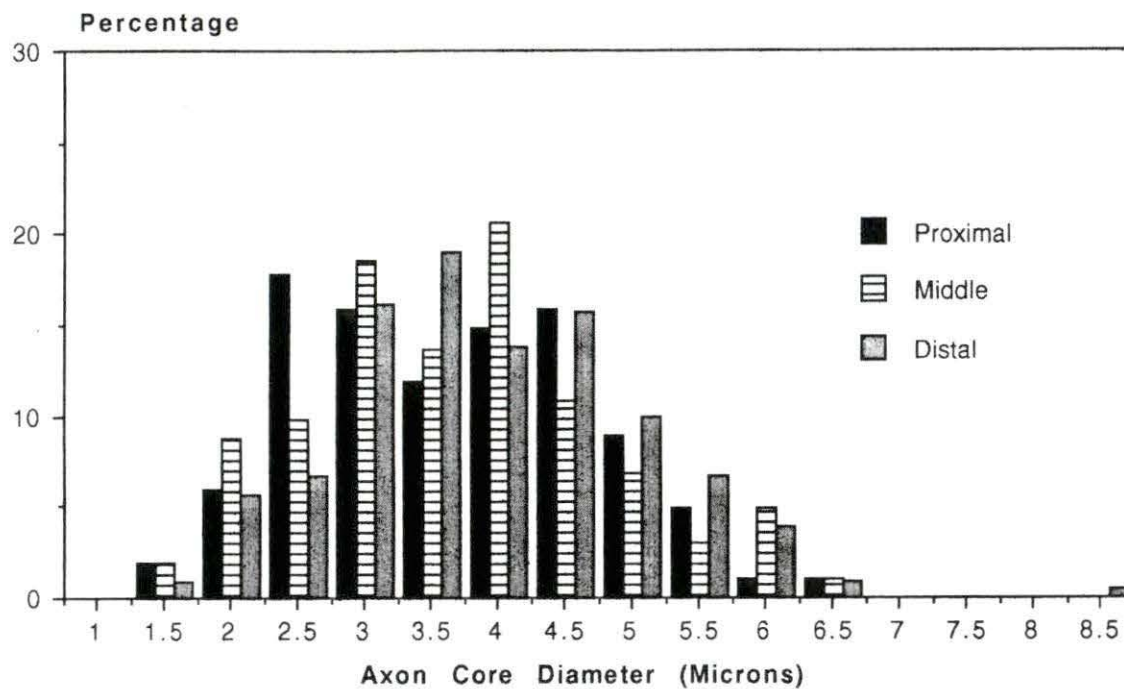
**Category II Axon Diameter Distribution  
 Animal #6, SEM  
 24 Weeks, Single-Lumen Cuff**



**Category II Axon Diameter Distribution  
Animal #47, SEM  
24 Weeks, Single-Lumen Cuff**

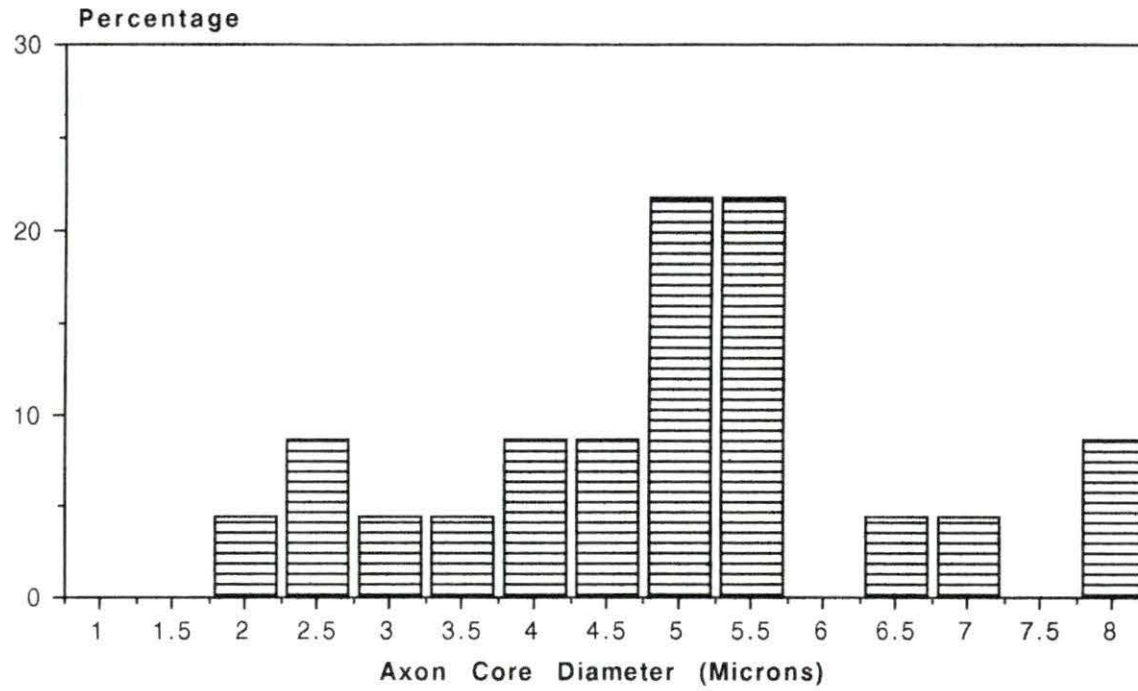


Category II Axon Diameter Distribution  
Animal #48, SEM  
24 Weeks, Single-Lumen Cuff

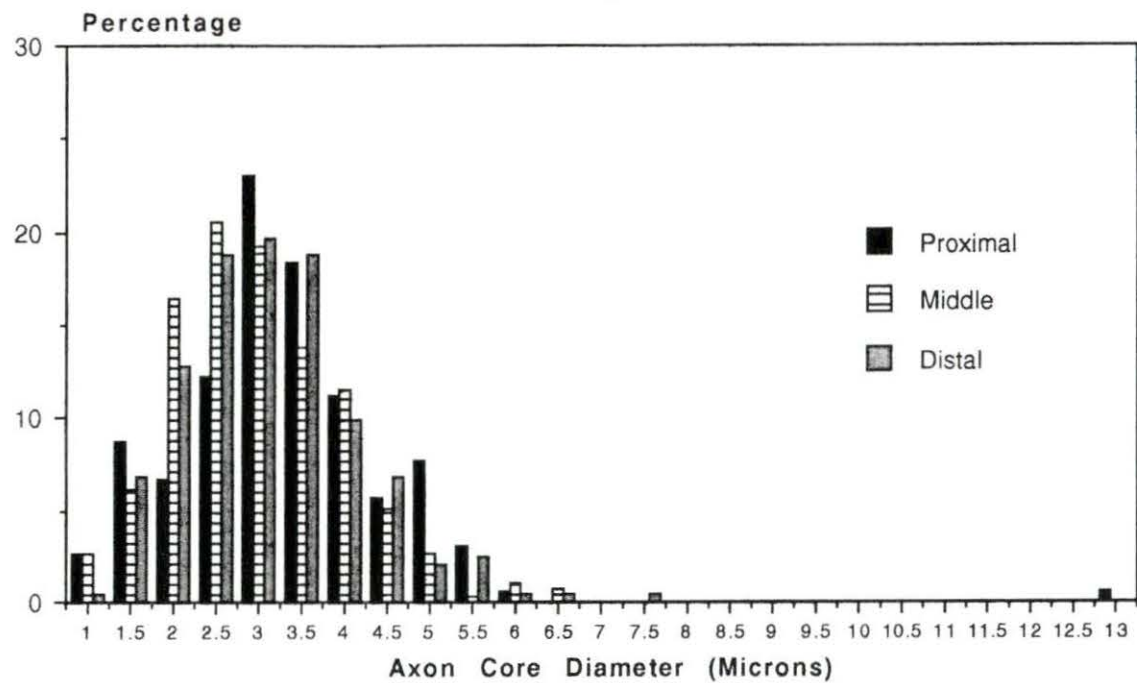




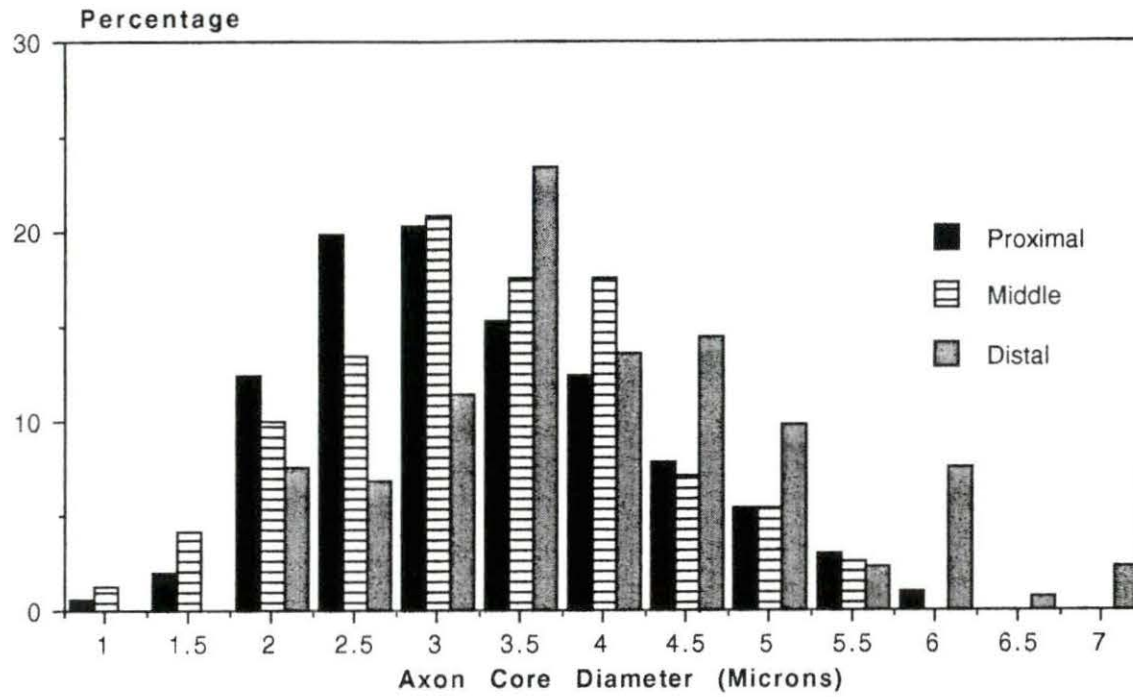
**Category II Axon Diameter Distribution  
Animal #9, SEM  
24 Weeks, Normal Control**



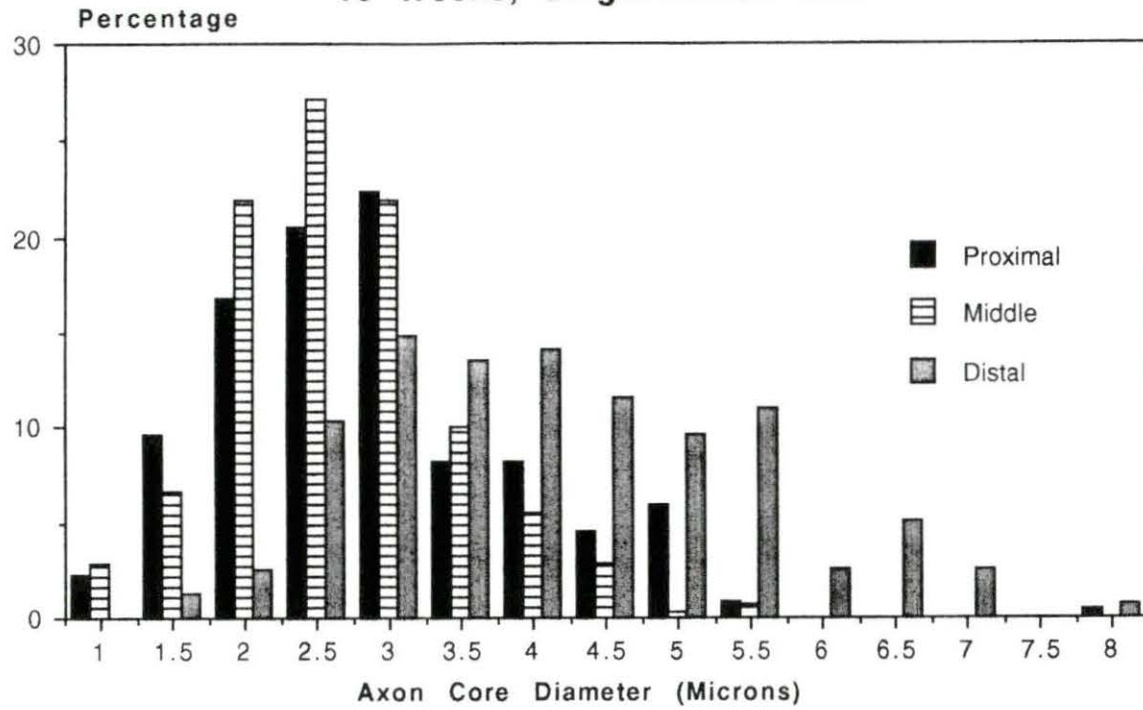
Total Axon Diameter Distribution  
Animal #41, SEM  
8 Weeks, Single-Lumen Cuff



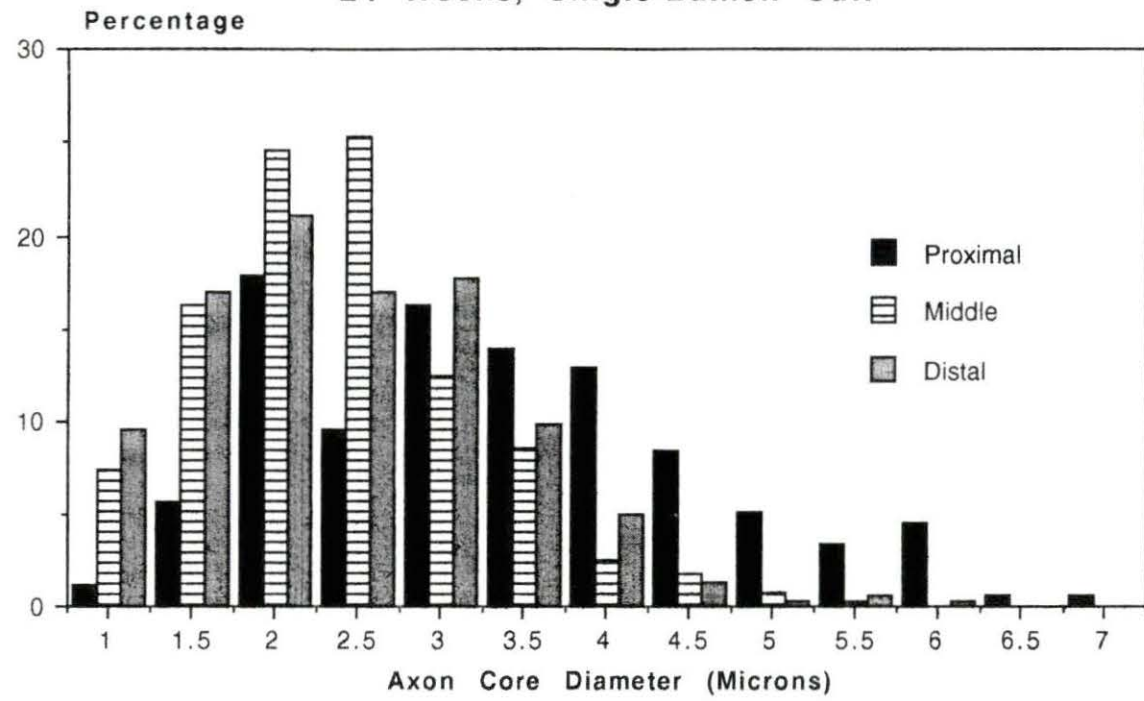
Total Axon Diameter Distribution  
Animal #43, SEM  
12 Weeks, Single-Lumen Cuff



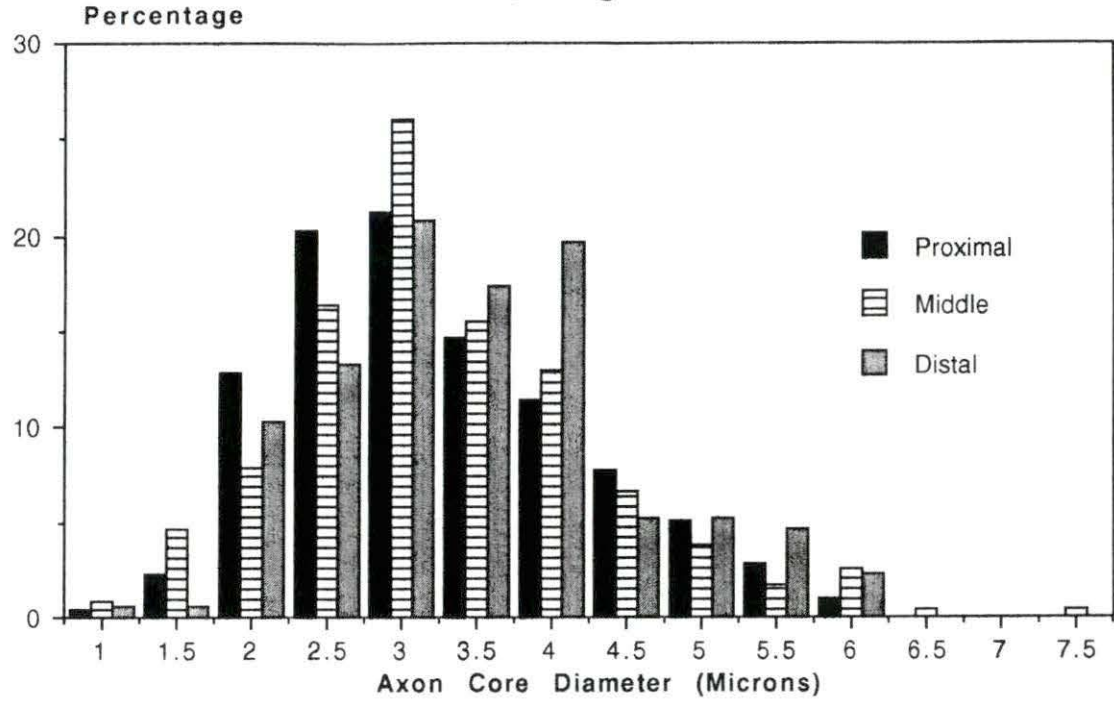
**Total Axon Diameter Distribution**  
**Animal #16, SEM**  
**16 Weeks, Single-Lumen Cuff**



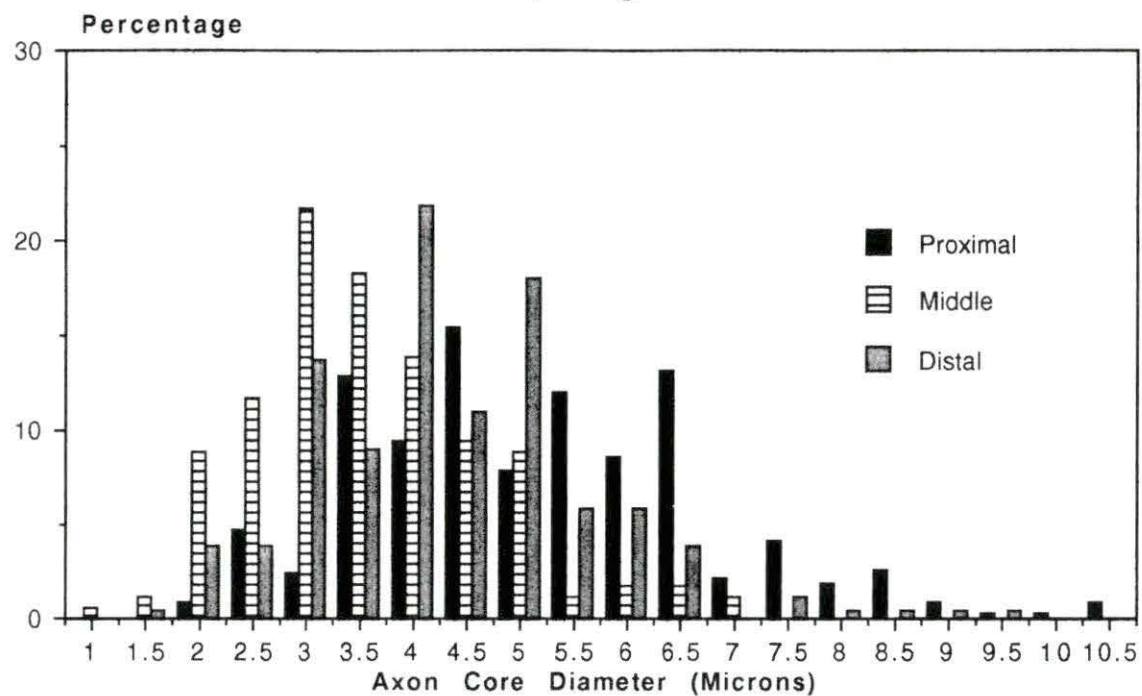
**Total Axon Diameter Distribution  
Animal #5, SEM  
24 Weeks, Single-Lumen Cuff**



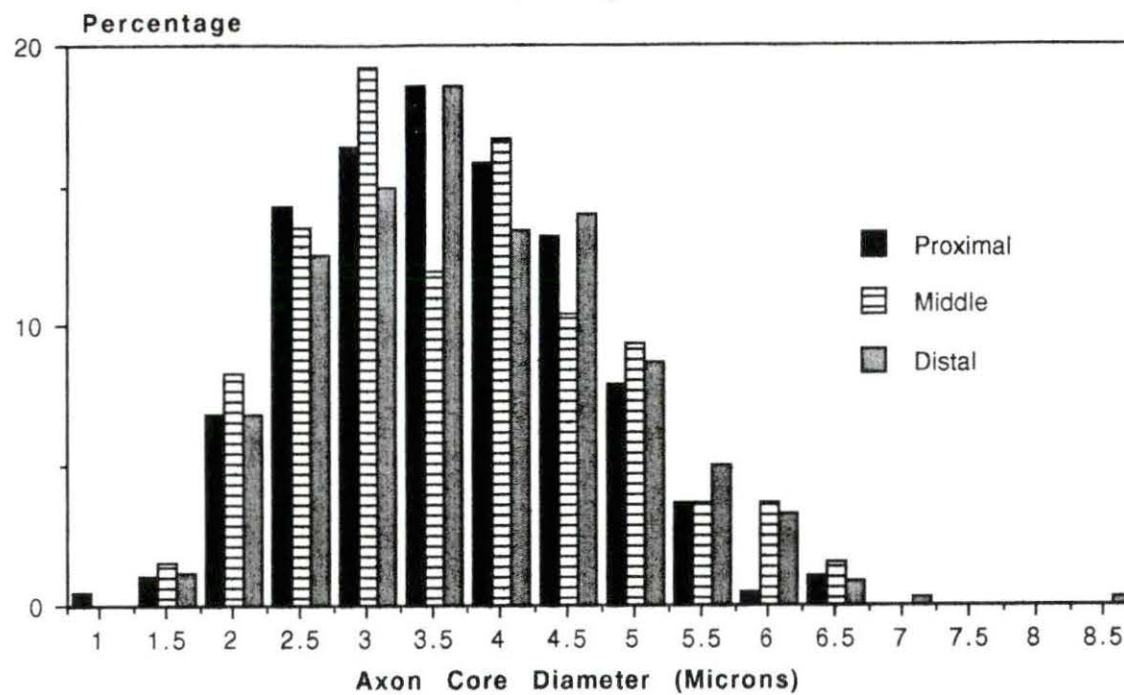
**Total Axon Diameter Distribution  
Animal #6, SEM  
24 Weeks, Single-Lumen Cuff**



**Total Axon Diameter Distribution  
Animal #47, SEM  
24 Weeks, Single-Lumen Cuff**



**Total Axon Diameter Distribution  
Animal #48, SEM  
24 Weeks, Single-Lumen Cuff**





**Total Axon Diameter Distribution  
Animal #9, SEM  
24 Weeks, Normal Control**

